R-10-36

Assessment of a KBS-3 nuclear waste repository as a plane of weakness

Margareta Lönnqvist, Ola Kristensson, Billy Fälth

Clay Technology AB

June 2010

Svensk Kärnbränslehantering AB
Swedish Nuclear Fuel
and Waste Management Co

Box 250, SE-101 24 Stockholm
Phone +46 8 459 84 00

ISSN 1402-3091
SKB R-10-36

Assessment of a KBS-3 nuclear waste repository as a plane of weakness

Margareta Lönnqvist, Ola Kristensson, Billy Fälth
Clay Technology AB

June 2010

This report concerns a study which was conducted for SKB. The conclusions and viewpoints presented in the report are those of the authors. SKB may draw modified conclusions, based on additional literature sources and/or expert opinions.

A pdf version of this document can be downloaded from www.skb.se.

Summary

The objective of this study is to investigate if the KBS-3 repository can act as a plane of weakness when subjected to different loads. These loads may cause either shear- or tensile fracturing. In this report these two modes of fracturing are simply referred to as “Shearing” and “Sheeting”, respectively.

The sensitivity of the rock mass to the presence of a system of tunnels is studied by means of numerical modelling using the two-dimensional distinct element code *UDEC*. In order to study the stability against shearing, the slip behaviours of two cases are compared:

- A single fracture embedded in a portion of rock.
- A single fracture embedded in a portion of rock is cutting through a system of tunnels, i.e. a repository.

The evaluation concerns three issues:

- How the presence of a system of tunnels affects the stability of the rock mass.
- How the presence of a system of tunnels affects the shear displacements in the hypothetical case of complete failure.
- How the tunnel spacing affects the stability and shear displacements.

The above is investigated for a number of *in situ* stress states. The stress states are varied in absolute magnitude, ratio between major and minor principal stress and inclination of the major stress with respect to the fracture plane.

The results from the models are used to evaluate the stability of the repository rock mass against shear failure in terms of Factor of Safety (FoS). The results indicate that the stability margin in the fracture has a limited sensitivity to the presence of the tunnels and to the tunnel spacing. Including tunnels with 40 m spacing gives a reduction of the stability margin by about 20% at a maximum. Applying the stress state where the stresses are oriented in order to give maximum instability gives a FoS higher than 1.4 for all tunnel spacings larger than 20 m.

The stability is also evaluated using stress input from dynamic earthquake simulations by /Fälth et al. 2010/. The FoS quantity is calculated based on the normal- and shear stresses recorded in horizontal planes in a M_w 6.2 model. The results indicate that even with a system of tunnels the rock mass have a high stability. Including tunnels with 40 m spacing at a location far from any fault edge, gives a FoS reduction from 4 to 3.5. Reducing the tunnel spacing down to 20 m gives a FoS of 2. In the earthquake model the earthquake is simulated using conservative assumptions (small rupture area, high fault slip velocity, large fault slip), which means that the stability evaluation here is conservative.

In order to study the stability against sheeting, a model with a number of fractures at different depths (10 m, 20 m, 30 m, 40 m, 50 m, 75 m, 100 m and 400 m) is subjected to a large horizontal stress increase. In order to provoke sheeting in the fractures, the model’s upper boundary simulates a curved ground surface, and all fractures are parallel with the ground surface. All fractures have zero tensile strength. After completed compression, sheeting is observed in all fractures down to 100 m depth. In the fracture at 400 m depth, the normal effective stress has been reduced from 6.5 to 6.0 MPa (about 8%). Thus, this fracture is still subjected to compressive stress. Given the conservative model assumptions (large horizontal compression, fractures at all depths parallel with the curved ground surface and zero fracture tensile strength), it can be concluded that there is no risk of sheeting failure at the projected repository depth (about 500 m). Since the rock mass will be subjected to vertical compression at all times at this depth, a system of tunnels will not give any increased risk of sheeting.

Based on the schematic and conservative modelling approaches applied here, it is concluded that, given the current repository layout with 40 m deposition tunnel spacing, the repository will not act as a plane of weakness. It is also concluded that a reduction of the tunnel spacing to 20–30 m will not increase the risk of shearing or sheeting at the repository depth.

Contents

1 Introduction

1.1 General

The concept for storing spent nuclear fuel applied by SKB is the KBS-3 system in which the spent fuel will be encapsulated in canisters consisting of a cast iron insert surrounded by a copper shell. The canisters will be deposited in vertical deposition holes in crystalline rock at approximately 500 m depth. They will be surrounded by a barrier of bentonite clay for isolation and mechanical protection (Figure 1-1).

SKB has decided to locate the deep repository for spent nuclear fuel at Forsmark in south-eastern Sweden. According to the proposed repository layout, the repository will require an area of about 3.6 km^2. The total rock volume to be excavated is estimated to $2.2 \cdot 10^6$ m^3 using a total tunnel length of about 70 km at the repository level, –470 m (Figure 1-2) /SKB 2009a/. The excavated volumes give an extraction ratio (area excavated/total area of repository) of less than 15%. This should be compared with the extraction ratios in mines which usually are more than 50% /Brady and Brown 1993/. As can be seen in the figure, the repository is divided into different deposition areas. The areas consist of numerous parallel deposition tunnels with 40 metres spacing. The height and width of the deposition tunnels are about 5 m and 4 m, respectively /SKB 2009a/.

It is well known within the engineering community that stress concentrations may arise around faults or imperfections inside a material when subjected to loading. Such stress concentrations can, if the stress intensity exceeds the fracture toughness of the material, lead to fracture propagation. Since the tunnel openings inside the deep repository can be considered as "faults or imperfections" inside the rock mass, it has been suggested that the repository itself may act as a plane of weakness that promotes large-scale fracturing of the host rock when subjected to future loads, and thereby jeopardizing its integrity /SKB 2003/.

Upon loading, rock fractures may reactivate either as Mode I (opening mode, e.g. sheeting), Mode II (in plane shearing mode, "sliding") or Mode III (anti-plane shearing mode, "tearing") /Atkinson 1987/. If large-scale fracturing takes place along the repository plane in response to a future load, the fracturing will follow one of these modes.

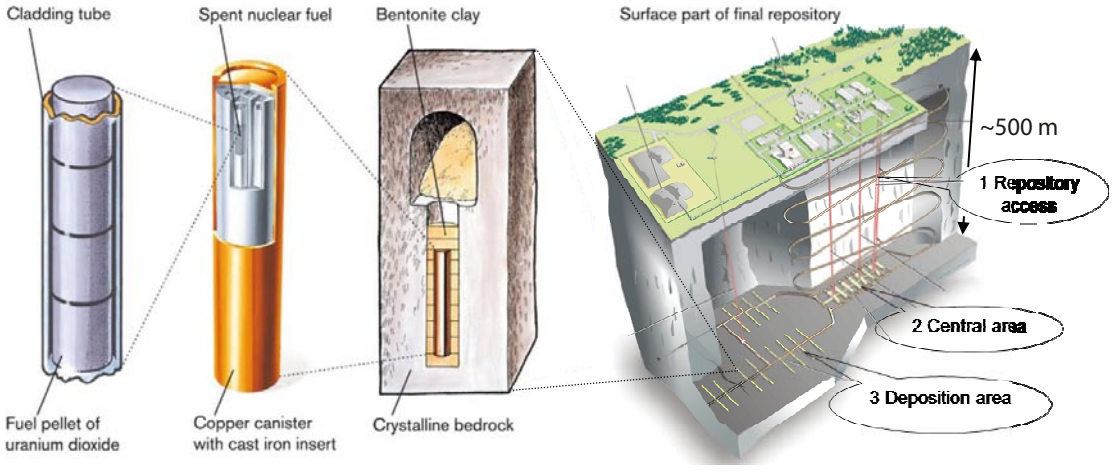

Figure 1-1. *Illustration of the KBS-3 concept for storing of spent nuclear fuel. The fuel is encapsulated in copper canisters which are deposited in vertical deposition holes at about 500 m depth in crystalline rock. The canisters are surrounded by a barrier of bentonite clay for isolation and mechanical protection. The tunnels are backfilled with bentonite clay in order to keep the bentonite buffer around the canisters in place and to inhibit water flows along the tunnels.*

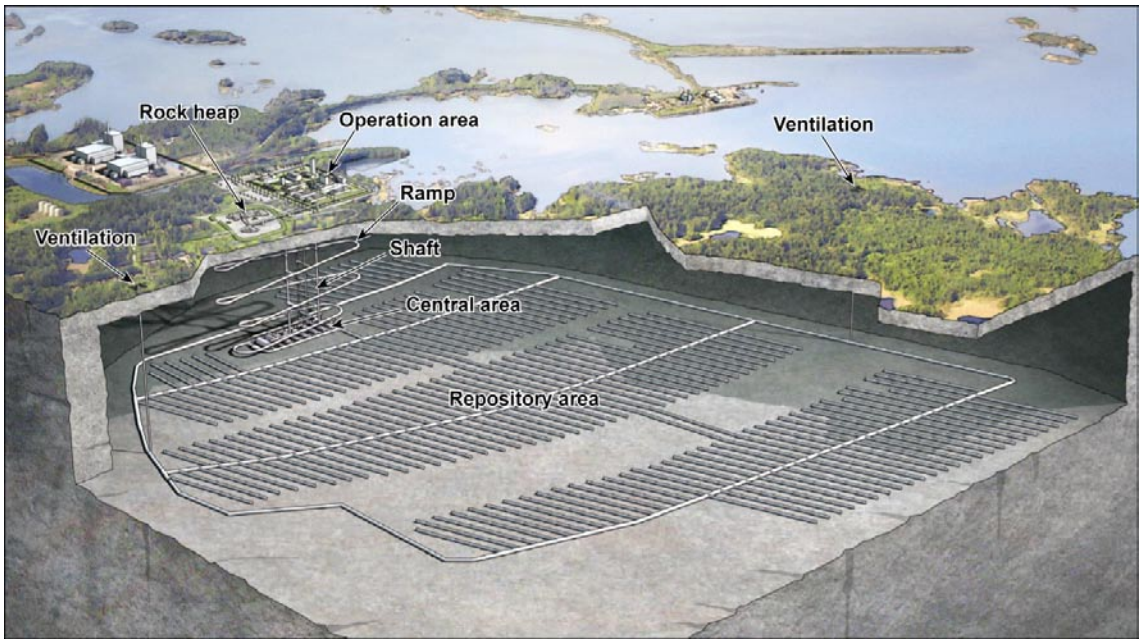

Figure 1-2. *General layout for the proposed repository at Forsmark. The total required tunnel length at the repository level is estimated to about 70 km. The repository is divided into different deposition areas, cf. /SKB 2009a/.*

1.2 Potential loads

There are a number of loads that the rock mass in the repository potentially may be subjected to, and for which one may consider the repository as a plane of weakness. These can be divided into two groups:

1. Induced loads: These are loads that are induced in the rock mass during construction of the repository and by subsequent processes that take place inside the repository after repository closure.
2. Natural loads: These loads are changes of the stress conditions in the repository host rock caused by e.g. glaciations or displacements in nearby rock faults.

1.2.1 Induced loads

Loads induced during construction

During the construction of the repository the excavation of tunnels and caverns will generate both dynamic loads (through blasting) and static loads (redistribution of *in situ* stresses, i.e. stresses that prevail in the rock mass before tunnel excavation). The blasting will introduce a region with an increased fracture density around the openings, the so called Excavation Damaged Zone (EDZ). The extension of this zone is of the order of one metre in the radial direction /Jonsson et al. 2009/. Figure 1-3a is a schematic that illustrates the shape and extension of the EDZ around a blasted test drift at the Äspö Hard Rock Laboratory.

The redistribution of *in situ* stresses leads to stress concentrations around the openings. It can be shown by means of analytical solutions (see e.g. /Brady and Brown 1993/) that the significant stress redistribution effect around a tunnel extends about two tunnel radii outside the tunnel wall. Depending on the *in situ* stress magnitudes, the orientation, shape and size of the opening, the stresses close to the opening walls may locally exceed the strength of the rock, with brittle failure (spalling) as a consequence (Figure 1-3b). The extent of spalling is dependent on the stress levels and the opening size. For a tunnel with 5 metre diameter the depth of failure may be of the order of 0.5 metre /Martin et al. 1999/. It can be concluded that the loads, both dynamic and static, induced by the construction of the repository are localised to regions close to the openings. Thus, these loads will not induce large-scale fracturing of the rock mass in the repository.

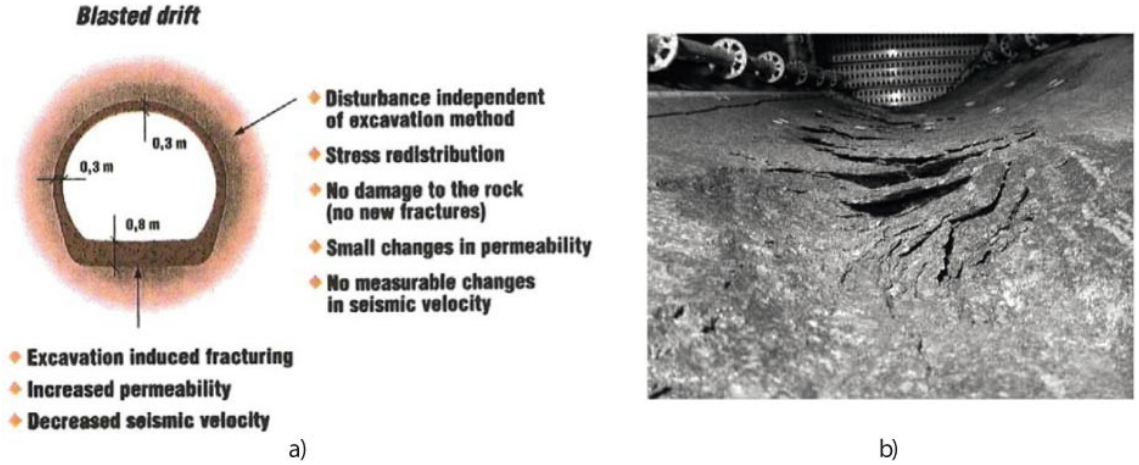

Figure 1-3. *a) Schematic that illustrates the EDZ around a tunnel excavated by blasting. The extension of the zone with increased fracture density is about 1 metre. From /Jonsson et al. 2009, Figure 3-3/. b) Brittle failure (spalling) at an opening wall in the Äspö Pillar Stability Experiment (APSE). From /Andersson 2007/.*

Loads induced by heating and swelling

The deposited spent nuclear fuel will generate heat. The heating power at the time of deposition is known as well as the power decay rate. The power of each canister will decay at a rate that depends on the burn-up of the fuel and the interim storage time, i.e. the time between discharge of the fuel from the nuclear power plant and deposition. This means that the rock temperature evolution as well as the corresponding thermal stress evolution can be predicted in detail, see e.g. /Probert and Claesson 1997, Ageskog and Jansson 1999, Ikonen 2005, Hökmark et al. 2010, Hökmark et al. 2009/.

At the very early stage of the heating period the rock around the deposition holes will be heated while the volumes between the tunnels remain at the initial temperature (Figure 1-4 top). Thus, one may consider the possibility that the expansion of the heated rock volumes surrounding the deposition tunnels is large enough to reduce the compression or even induce tensile stresses in the cold, non-expanding volumes between the tunnels. It is however shown by thermo-mechanical calculations /Hökmark et al. 2010/ that, during this early stage, the effects of the heating on the vertical stresses between the tunnels are modest. The diagram in Figure 1-5 shows the simulated temporal developments of the effective normal stresses, i.e. the total stress minus the hydrostatic pore pressure, in a number of points in a horizontal fracture 3 m below the deposition tunnel floor. The effective stress at point E, which is located between the tunnels, is reduced a few MPa during the first years of heating, but is above 5 MPa at all times.

A similar stress reduction effect is found at later stages, but at a larger scale. The expanding rock within the deposition areas will work as to lift the rock lying above. The rock volumes between the deposition areas as well as the rock outside the repository will have lower temperatures and will expand less. Thus, the vertical compressive stresses in these rock volumes will be reduced (Figure 1-4 bottom). However, these vertical stress reductions amount to 4–5 MPa at repository depth after about 100 years (Figure 1-6), and since the vertical *in situ* effective stress is about 8 MPa /Glamheden et al. 2007/, the stresses remain compressive at all times. Thus, there is no risk of large-scale fracturing. In addition, inside the heated repository areas, which here are assessed as potential areas of weakness, the rock mass is also subjected to compressive stresses at all times, as discussed above.

Another effect of the heating is that the tangential stresses around the openings (tunnels and deposition holes) will be increased. This may induce spalling at locations where the stresses exceed the rock's spalling strength. However, similarly to the brittle failures that may result from the excavation of the openings (see above), these are very local effects.

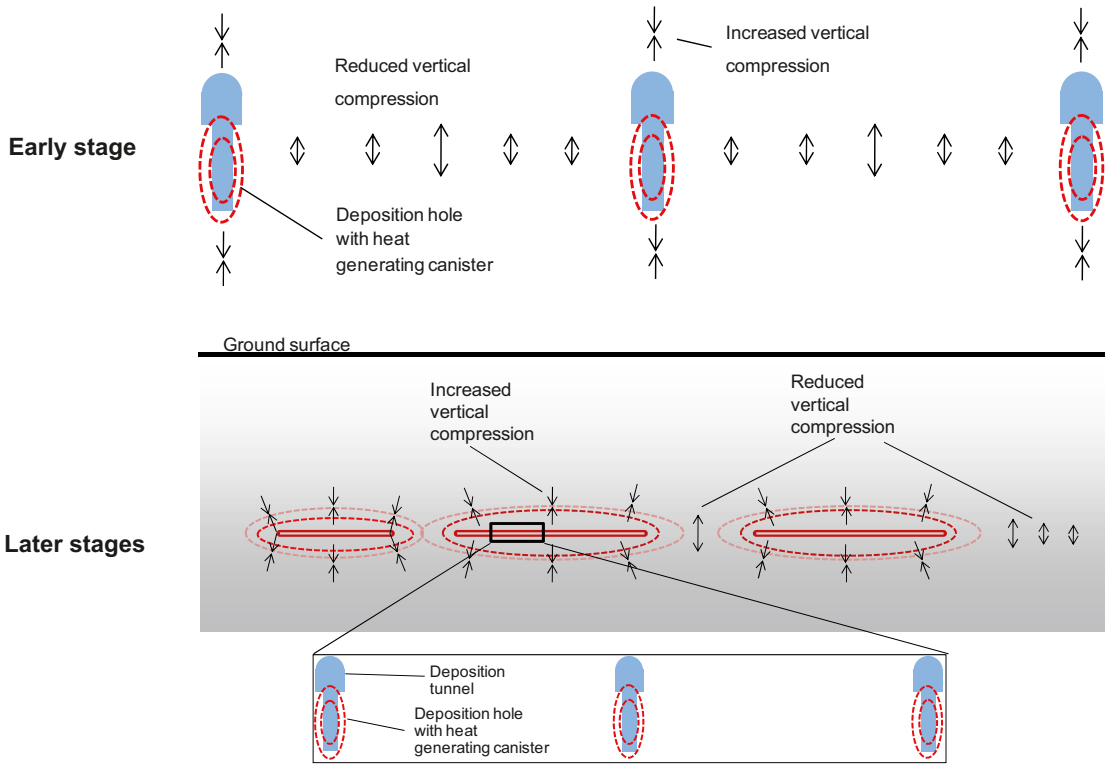

Figure 1-4. *Schematic sketch of a vertical section through the repository illustrating the effects on vertical compressive stresses caused by the heat generating spent fuel. Top: Reduction of vertical stresses between deposition tunnels during the early stage of the heating period. Bottom: Stress reductions in the regions between deposition areas during later stages of the heating period.*

The bentonite clay, which will be surrounding the copper canisters and which will be used as tunnel backfill, will swell as it takes up water from the host rock and thereby exert a swelling pressure at the walls of the rock openings. The swelling pressure will be in the range 5–10 MPa /SKB 2010a/. Since the *in situ* stresses are considerably higher, these pressures will only have very local effects on the stress situation around the rock openings. The two horizontal principal *in situ* stress components at the planned repository depth (–470 m) in Forsmark are about 40 MPa and 20 MPa, respectively. The vertical stress component, which corresponds to the rock overburden, is about 12 MPa /Glamheden et al. 2007/. The swelling pressure may give small tensile stresses close to deposition tunnel walls /Hökmark et al. 2010/, but this will not lead to any large-scale fracturing since it is a local effect.

1.2.2 Natural loads

Sheeting

Sheeting joints (or "exfoliation" joints) are fractures that form parallel or sub-parallel to the topographic surface /Bahat et al. 1998, Mandl 2005/. Consequently these sheeting joints are normally found at relatively shallow depths. They are often gently curved, but with increasing depth they usually become more horizontal. Sheeting joints are preferably found in strong rocks, such as granite, gneiss, massive sandstone and marble /Jahns 1943, Martel 2006/. /Jahns 1943, Martel 2006/ suggest that sheeting joints develop due to tensile stresses normal to the topographic surface caused by high horizontal stresses. In order to develop tensile stresses large enough for joints to open up, the rock mass must be able to withstand high compressive stresses in the horizontal direction. According to /Martel 2006/, the combination of a strong rock mass with high horizontal stresses and a curved (convex) topographic surface is a prerequisite for sheeting joints to develop (Figure 1-7). Sheeting joints may be found also at sites where the stresses are too low or where the surface curvature is too small for sheeting joints to develop. There are two possible explanations to this: First, the regional stress levels may have been reduced since the time when the jointing took place. Second, the surface curvature may have been larger when the joints developed but has since then been reduced due to erosion /Martel 2006/.

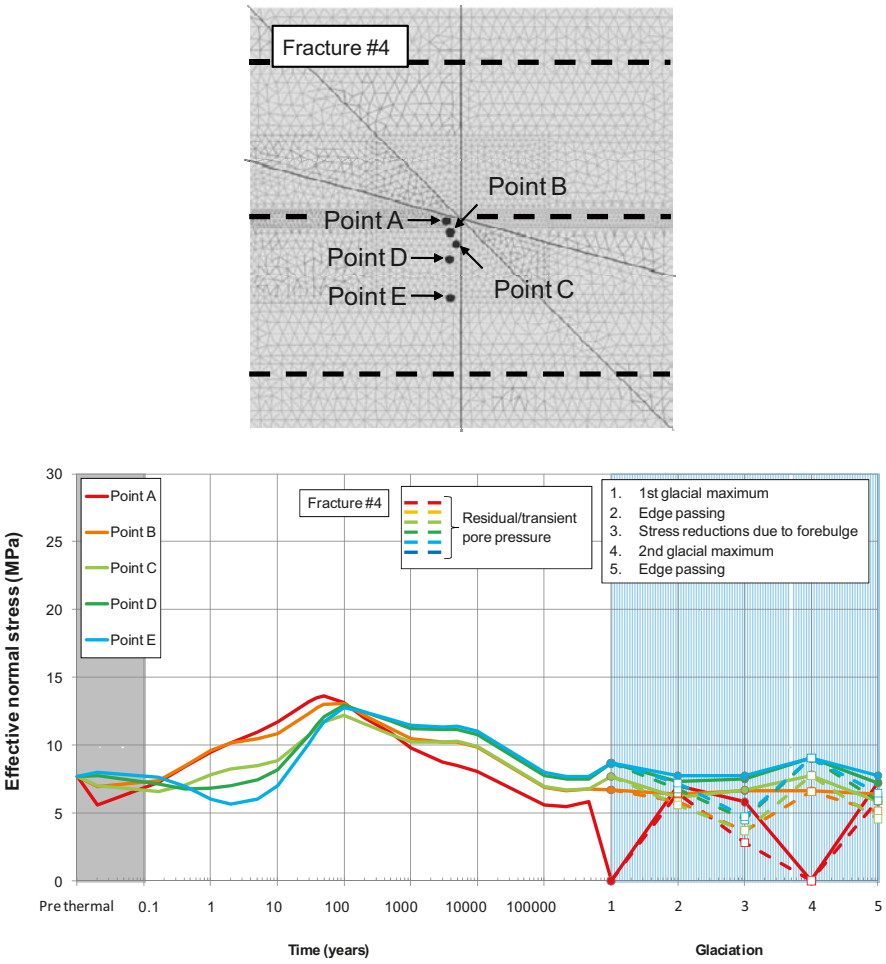

Figure 1-5. *Top: Location of history points in a horizontal fracture 3 m below deposition tunnel floor in 3DEC model. The dashed lines indicate location of tunnels. Bottom: Temporal development of effective normal stress at different locations in the fracture. The fracture is in a compressive state during the entire heating period. From /Hökmark et al. 2010/.*

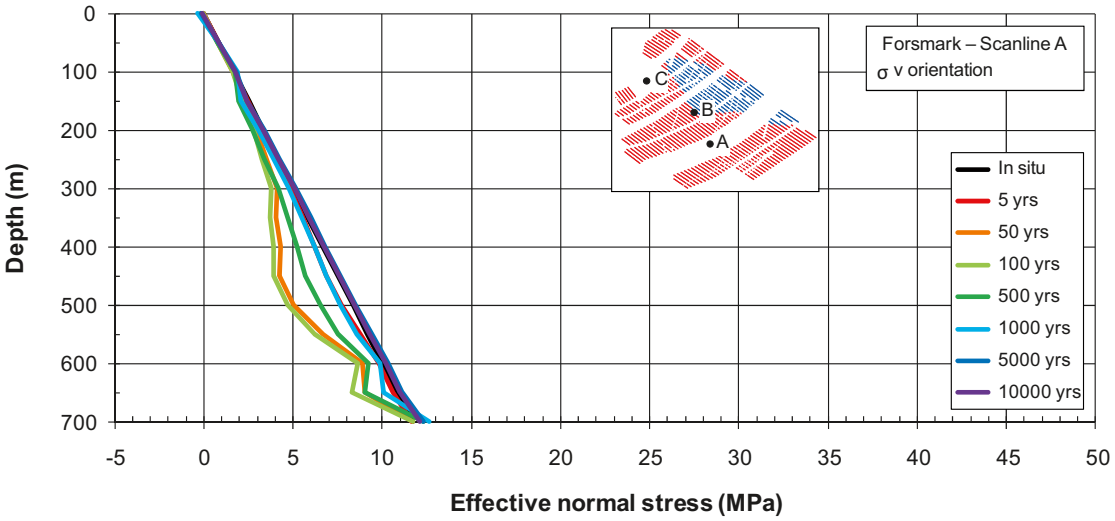

Figure 1-6. *Results from large-scale thermo-mechanical model /Hökmark et al. 2010/. Effective normal vertical stress along vertical scan-line A between deposition areas as shown by the inset.*

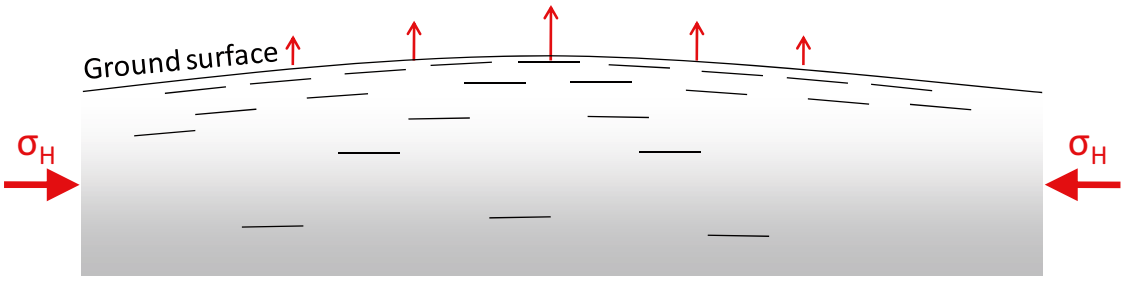

Figure 1-7. *Schematic of sheeting joints in a vertical cross section. The joints develop due to a combination of high horizontal stresses and a curved ground surface.*

Down to about a maximum depth of about 200 metres at the Forsmark site, there is a relatively high frequency of sub-horizontal and gently dipping fractures. It is suggested that unloading related to removal of sediments or ice-sheets resulted in reactivation of gently dipping ancient fractures and also creation of new fractures (sheeting joints) /Stephens et al. 2007/ (cf. Figure 1-8). During glaciation, the weight of the ice will cause the crust to bend down. The compressive flexural stresses generated in the upper parts of the crust will add to the existing horizontal stresses. When the ice cover and its associated vertical stress loads disappear, the coupling between the lower crust and the viscous mantle will delay the isostatic rebound of the deformed crust. The result is that components of the glacially-induced horizontal stresses could remain /Lund et al. 2009/ and may, if the topography and fracture array is favourable, cause sheeting joints.

One may consider the theoretical possibility that the repository acts as a plane of weakness that could promote large-scale horizontal fracturing of the bedrock at repository depth in connection with the retreat of future ice covers. This is schematically illustrated in Figure 1-9. This load case is studied in Section 5.2.

Hydraulic jacking

Hydraulic jacking is a phenomenon that occurs when the pore pressure in a fracture exceeds both the normal stress acting on the fracture and the fracture's tensile strength. Sub-horizontal fractures, which may have been created by hydraulic jacking, have been found at shallow depths at the Forsmark site (cf. Figure 1-8).

Figure 1-8. *Shallow fractures sub-parallel to the ground surface in the excavation for unit 3 of the Forsmark power plant /Carlsson 1979/. The fractures may have been created by extensional strains caused by large horizontal loads (sheeting joints). They may also have been formed or opened up further by high pore pressures (hydraulic jacking).*

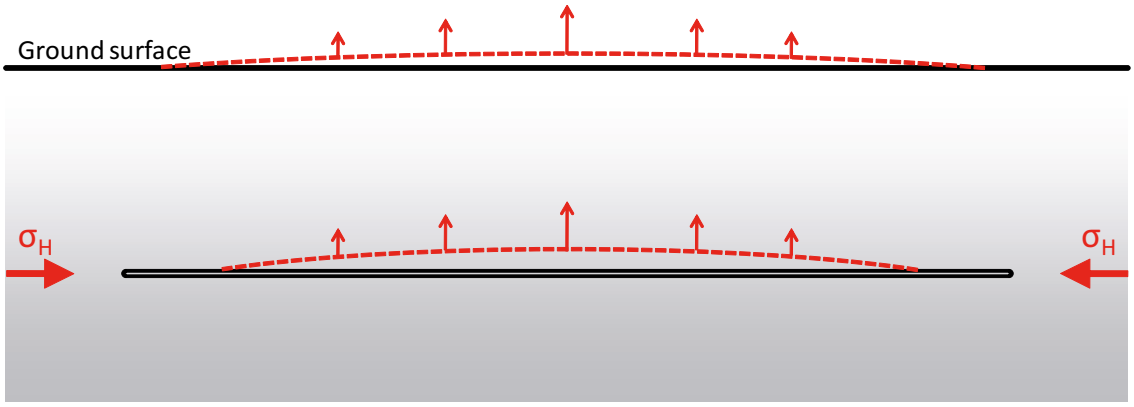

Figure 1-9. *Schematic sketch illustrating the theoretical possibility that the repository acts as a plane of weakness that promotes large-scale fracturing of the bedrock in response to high horizontal stresses.*

One may consider the repository as a plane of weakness that promotes hydraulic jacking at repository depth. If the pore pressure within the repository is increased to high levels, there would be a theoretical risk of jacking. The loading conditions that could come in question for this process are those that can be found when a glacial ice sheet is approaching the repository site or at the end of a glaciation when the vertical ice load disappears. In both these cases, the pore water pressures may be increased in the bedrock /Chan et al. 2005, Lönnqvist and Hökmark 2010/. The question is if there is any possibility that the pore pressure at repository depth can be increased such that it exceeds both the weight of the rock overburden and the strength of the bedrock. /Lönnqvist and Hökmark 2010/ have carried out extensive numerical modelling studies in order to assess the possibility of hydraulic jacking at different depths. They studied numerous cases including different assumptions of ice approach/retreat speed, permafrost and bedrock hydraulic properties. Based on schematic and conservative assumptions, they conclude that glacially-induced hydraulic jacking may only take place at depths between 0 and 200 metres. Thus, there is no risk of hydraulic jacking at repository depth.

Shearing

Since the principal *in situ* stress components are vertical and horizontal, respectively, /Glamheden et al. 2007/ there are no shear stresses along the repository (i.e. the horizontal) plane at present day conditions. This will also be the case during the heating period following repository closure since the thermal stress components also will be aligned to the horizontal plane /Hökmark et al. 2010/. However, shear loads on the repository scale could potentially be induced by stress redistributions that are caused by movements in nearby rock faults (Figure 1-10) or by glacial loads. This load case is studied in Section 5.1.

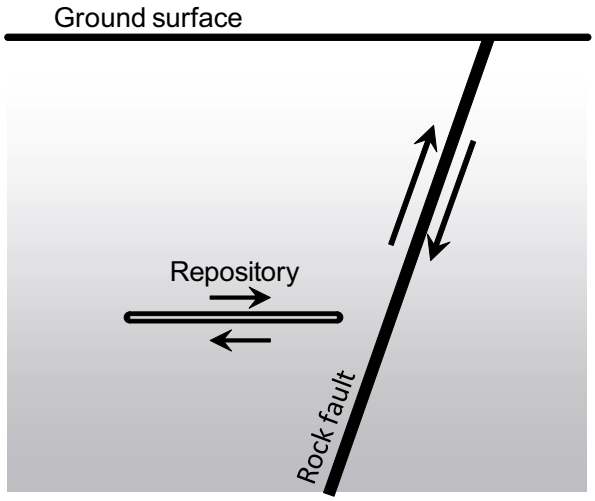

Figure 1-10. *The sketch illustrates how movements in nearby rock faults potentially could induce shear stresses along the repository plane.*

1.2.3 Summary

In this section a number of potential loads that the repository rock may be subjected to have been discussed. The induced loads are mechanical and thermo-mechanical loads caused by the construction of the repository, by the heat generating spent fuel and by swelling pressure from the bentonite clay that will be used as buffer and backfill in the repository. The natural loads that have been discussed are high pore pressures that might induce hydraulic jacking, sheeting caused by large horizontal loads and shear loads that may be induced by nearby fault movements or glaciations.

Based on the results from the other studies referred to in this chapter it can be concluded that, for the majority of the loading cases, there is no risk that the repository could act as a plane of weakness that promotes large-scale fracturing. However, two load cases are identified that cannot be disregarded based on results from other studies. These two load cases could theoretically induce sheet- and shear fractures in the repository. Therefore, the work presented in this report is focused on these two cases.

2 Objectives

The objective of this study is to investigate if the KBS-3 repository can act as a plane of weakness when subjected to different loads. These loads may cause either shear- or tensile fracturing. In this report these two modes of fracturing are simply referred to as “Shearing” and “Sheeting”, respectively. The study is carried out by means of two-dimensional numerical modelling.

2.1 Shearing

The evaluation concerns three issues:

- How the presence of a system of tunnels affects the stability of the rock mass.
- How the presence of a system of tunnels affects the shear displacements in the theoretical case of complete failure.
- How the tunnel spacing affects the stability and shear displacements.

The above is investigated for a number of stress states. The stress states are varied in absolute magnitude, ratio between major and minor principal stress and inclination of the major stress with respect to the fracture plane.

2.2 Sheeting

The sheeting problem is addressed by the study of the normal stresses in a number of fractures at different depths in a rock mass that is subjected to a large horizontal stress increase. The fractures are given a geometry that promotes sheeting.

3 Investigation procedure

3.1 Shearing

In order to simplify the numerical analysis, formation and propagation issues are circumvented by assuming that there exists a hypothetical fracture cutting through the repository at tunnel mid-height. To compare stress magnitudes and displacements a model encompassing a portion of rock with a single fully embedded fracture is run alongside the models with tunnels. Figure 3-1 shows a conceptual model of the problem. The tunnels dimensions as well as the base case assumption for the tunnel spacing are in accordance with the projected repository /SKB 2009a/ (cf. Section 1.1). The models, which are to be compared, are subjected to the same initial stress state (σ_{xx}, σ_{yy}, σ_{xy}). The study is carried out using 2D-models, which means that the tunnels and the fracture are assumed to have infinite extensions in the out-of-plane direction. This assumption rather overestimates than underestimates the influence of the tunnels, and is thus conservative.

The influence of the presence of the tunnels is investigated by studying the stresses and displacements along the fracture plane. The stability of the rock mass is evaluated in terms of the Factor of Safety (FoS). The FoS quantity is calculated based on the normal- and shear stresses in the fracture in the initial state, i.e. before fracture slip.

In addition to the static 2D-model results provided here, numerical results from dynamic earthquake simulations by /Fälth et al. 2010/ are used to evaluate the stability.

3.2 Sheeting

The potential for sheeting at repository depth is studied by use of a model with the conceptual geometry shown in Figure 3-2. In order to simulate a curved surface topography, the middle section of the model's upper boundary is bent upwards. A number of fractures are included in the middle section at different depths. The fractures are sub-horizontal and have the same shape as the inclined ground surface. The fracture strength parameter values are in accordance with Forsmark site data for the rock mass. *In situ* stresses are applied and then the vertical boundaries are moved towards the model centre in order to increase the horizontal stresses. The normal stresses in the fractures are studied as the horizontal stresses are increased. A fracture with zero normal stress is regarded as a sheet joint. The idea here is to compare the potential for sheeting at shallow depths (<100 m) with the potential at repository depth (> 400 m).

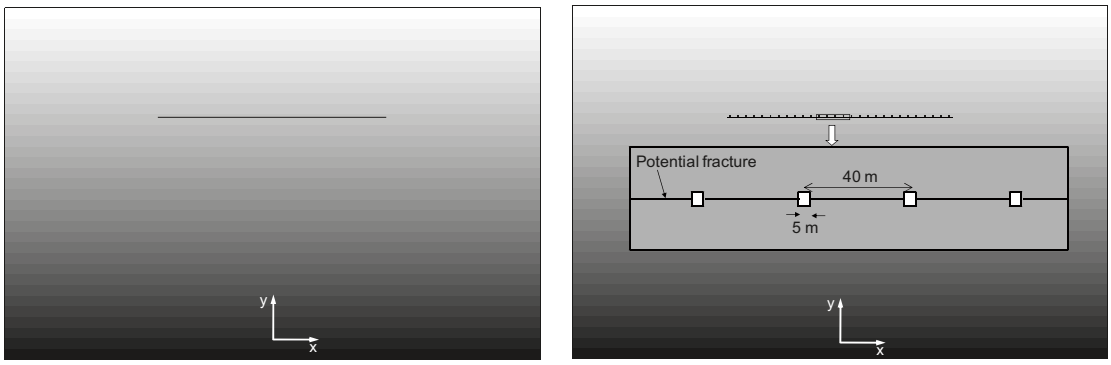

Figure 3-1. *Illustration of conceptual models: a) model with a fracture only and b) model with a fracture cutting through a number of square voids representing the tunnels in the repository. The tunnels dimensions as well as the base case assumption for the tunnel spacing are in accordance with the projected repository /SKB 2009a/.*

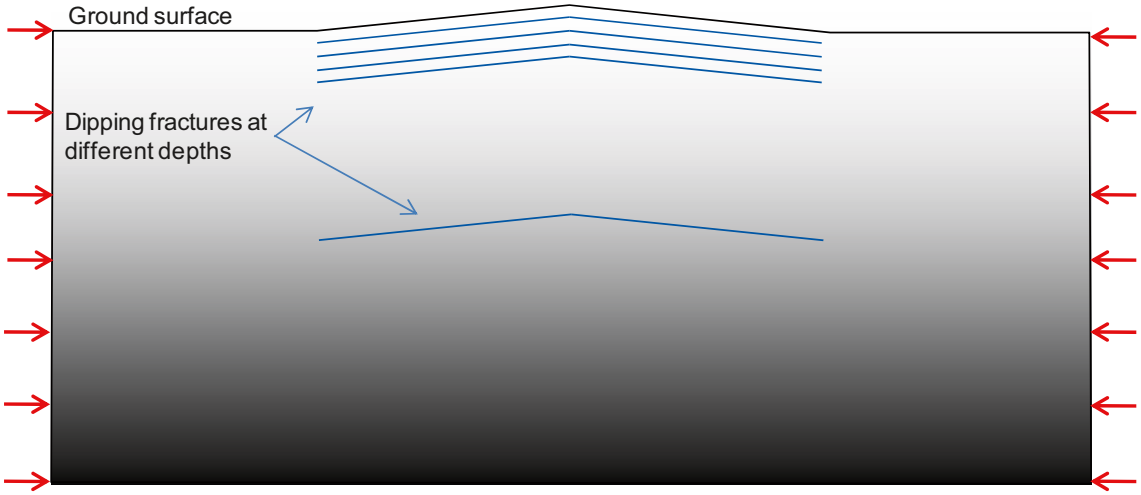

Figure 3-2. *Conceptual 2D-model geometry used to study the potential of sheeting at repository depth. Sheeting was simulated in fractures at different depths by an increase of the horizontal stresses.*

4 Model description

In this section, descriptions of the numerical models are given. The numerical tool, model geometries, constitutive laws, parameter values, initial- and boundary conditions are presented. One subsection presents the shear load case model and another subsection presents the sheeting model.

4.1 Description of the numerical tool

The models are analysed by use of the two-dimensional program *UDEC* (Universal Distinct Element Code). *UDEC* simulates the response of discontinuous media (such as jointed rock masses) subjected to either static or dynamic loading. The code employs an explicit time-stepping solution scheme. The discontinuous medium is represented by an assemblage of discrete blocks. The discontinuities are treated as boundary conditions between the blocks; large displacements along discontinuities and rotations of blocks are allowed. Individual blocks behave either as rigid or deformable material. Deformable blocks are subdivided into a mesh of finite-difference elements, and each element responds according to a prescribed linear or non-linear stress-strain law. The relative motion of the discontinuities is also governed by linear or non-linear force-displacement relations for movement both in the normal and shear directions. *UDEC* is based on a "Lagrangian" calculation scheme that is well-suited to model the large movements and deformations of a blocky system /Itasca 2005/. The code documentation contains several examples that verify the performance of the program. For further reading about the distinct element method, see e.g. /Jing and Stephansson 2007/.

4.2 Model for study of the shear load case

4.2.1 Geometry

The geometry for the fracture subjected to shear loading is shown in Figure 4-1. The model has a plane rectangular geometry of the considered rock mass with outer dimensions 3,480 m x 1,392 m. In the rock mass a fracture with a total length of 1,160 m is symmetrically positioned. The length of the fracture is based on a generic repository layout that was available at the time of model setup. In that layout, there were about 30 deposition tunnels (29 tunnel spacings) in each deposition area (29 x 40 m = 1,160 m). It shall be noted that the exact length of the fracture has no importance for the results.

The repository is schematically represented by a number of square voids which represent the tunnels. The voids have a side length of 5 m, which is in accordance with the dimensions of the deposition tunnels in the proposed repository (cf. Section 1.1). The tunnels are positioned symmetrically in the model with, in the base case version, a 40 m centre to centre distance as shown in Figure 4-2. In order to determine the sensitivity to tunnel spacing, a number of models with smaller tunnel spacing are run. In each model, the number of tunnels is determined by the length of the fracture (1,160 m) and the tunnel spacing, e.g. the model with 10 m tunnel spacing has 117 tunnels.

The geometry has been discretized using triangular constant strain elements. In the area close to the fracture and tunnels, the largest element edge length is prescribed to 1.25 m. The element dimension increases with increasing vertical distance from the fracture (see Figure 4-3).

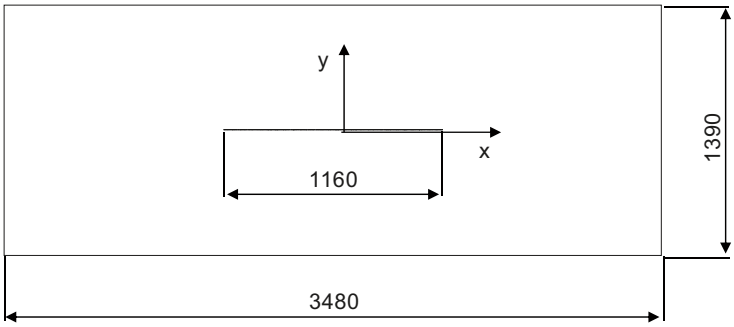

Figure 4-1. *Model geometry. The fracture is located in the middle of the model. The fracture length is based on the assumption that there will be 30 deposition tunnels (29 tunnel spacings) in a deposition area.*

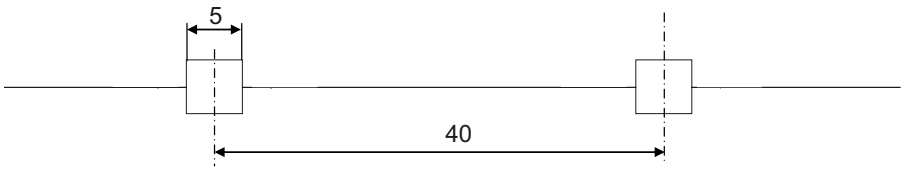

Figure 4-2. *Tunnel geometry. The repository is schematically represented by a number of square voids. The reference tunnel spacing is 40 m.*

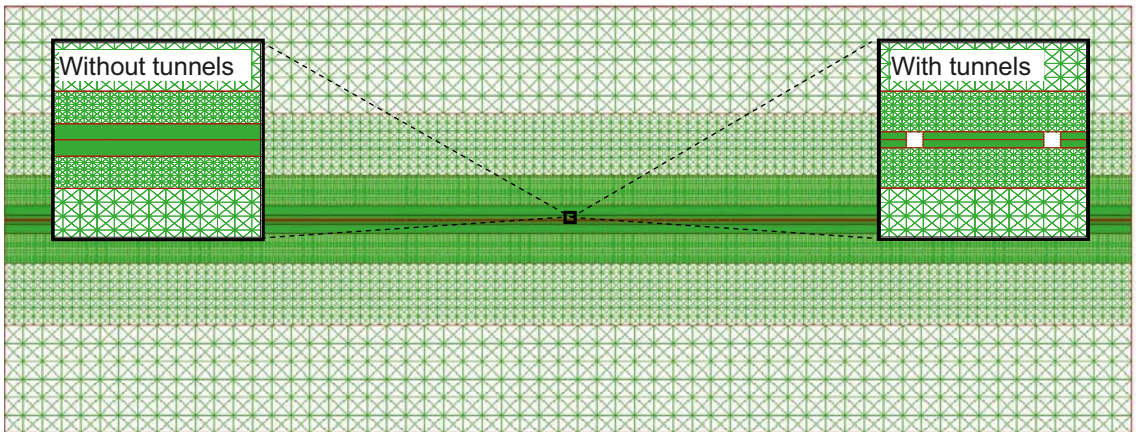

Figure 4-3. *UDEC model geometry showing the triangular constant strain elements. Insets show close ups of the model geometry without tunnels (left) and with tunnels (right).*

4.2.2 Constitutive models

The rock mass is assumed to be linearly elastic, isotropic, homogenous and continuous. The fracture is assumed to respond to loads according to an idealised elasto-plastic material model with linear joint stiffness and shear failure according to a Coulomb criterion (Figure 4-4). The cohesion, c, is set to zero at shear failure. In this analysis, the pore pressure, P, is set to zero. The parameter values are set according to Table 4-1.

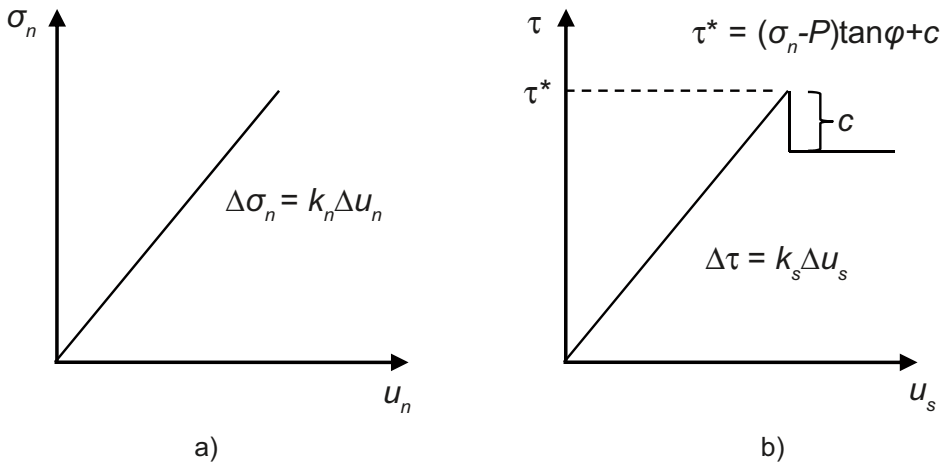

Figure 4-4. *Idealised elasto-plastic material model with linear joint stiffness and shear failure according to a Coulomb criterion. a) Linear relation between the fracture normal stress, σ_n, and the normal displacement, u_n. b) Linear relation between the fracture shear stress, τ, and the shear displacement, u_s. The cohesion, c, is set to zero at shear failure.*

Table 4-1. Material property parameter values.

	Parameter	Value	Unit
Continuum	Young's modulus, *E*	68	GPa
	Poisson's ratio, *υ*	0.22	–
	Density, *ρ*	2,700	kg/m^3
Fractures	Normal stiffness, k_n	1,500	GPa/m
	Shear stiffness, k_s	500	GPa/m
	Friction angle, *φ*	35	deg
	Cohesion, *c*	Different values	MPa

4.2.3 Stress states

Two different principal stress combinations have been used:

σ_1 = 50 MPa, σ_2 = 10 MPa, and,

σ_1 = 70 MPa, σ_2 = 10 MPa.

Note that here, the compressive stresses are positive. In order to specify the stress state, an angle, α, is introduced. The angle is defined as the angle between the major principal stress, σ_1, and the fracture plane. The correlation between the principal stresses, σ_1 and σ_2, the angle, α, and the resulting shear stress, τ, in the fracture plane is shown in Figure 4-5.

4.2.4 Boundary conditions

To prescribe suitable boundary conditions, the distinct element model is embedded in an infinite elastic medium with the same elastic properties as the rock itself. This is obtained by using a feature in *UDEC* where a coupling between boundary elements and the distinct element model is provided.

Boundary elements have been used in order to reduce the influence from the conditions acting on the boundary and, as a consequence, to be able to reduce the dimensions of the model. If alternative boundary conditions, such as a prescribed stress vector field or a displacement field, are used, the model demands greater dimensions in order to compensate for too weak or too stiff conditions as compared to the actual *in situ* state. The chosen stress state is applied over the entire structure and plane strain conditions are adopted.

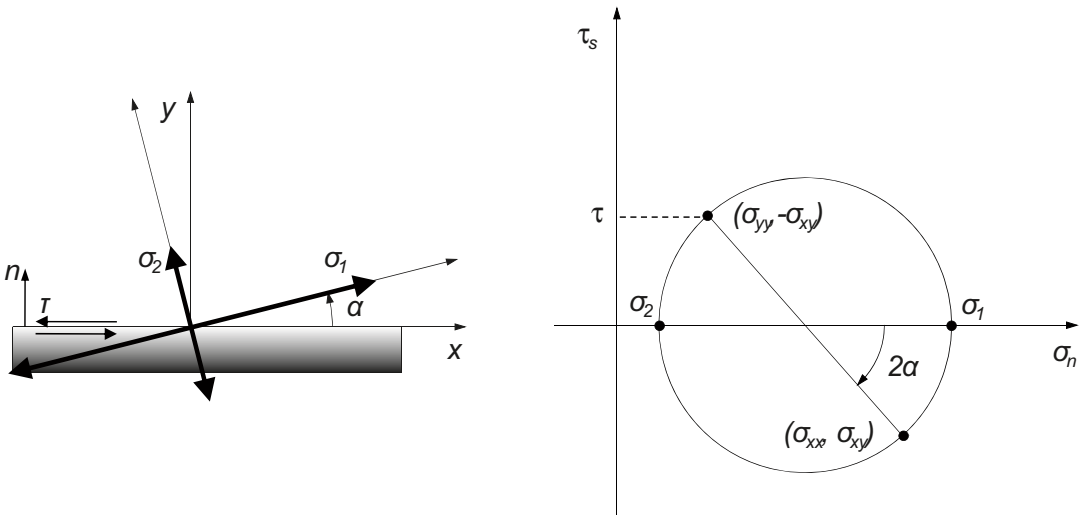

Figure 4-5. *The correlation between the principal stresses, σ_1 and σ_2, the angle, α, and the resulting shear stress, τ, in the fracture plane.*

4.2.5 Case overview

An overview of the studied cases is presented in Table 4-2. Regarding the model geometry, there are two basic assumptions: No repository and repository with 40 m tunnel spacing. In addition, there are models with alternative tunnel spacings (10 m, 15 m, 20 m and 30 m), which means that there are totally six model geometries. These geometries are combined with four different states of stress.

The stress states are exaggerated in the sense that the repository is unlikely to be subjected to quasi-static stress loads with these large stress anisotropies. During a future ice age, for instance, a passing ice front will introduce some anisotropy to the stress field, but it is not likely to possess the magnitudes of the prescribed stress states in these numerical models. The largest shear stress induced in the fracture plane in Case 3 is 30 MPa, whereas the maximum glacially-induced shear stress at the Forsmark site is estimated to have been less than 10 MPa during the latest glaciation /Lund et al. 2009/.

4.3 Model for study of the potential for sheeting

4.3.1 Geometry

The outline and dimensions of the model are shown in Figure 4-6. The model represents a portion of rock. The upper boundary represents the ground surface. In order to represent a curved ground surface which promotes the development of sheeting joints, the mid-point of the ground surface is shifted 15 m in the positive y-direction. The "curved" part is 1,000 m wide. This gives a 1.7° inclination of the surface in both the positive and negative x-directions. Within the region located below the "curved" part of the boundary, a number of fractures are included at different depths. The fractures are parallel to the upper boundary (ground surface) and thus have the same inclination. The fractures are located at 10, 20, 30, 40, 50, 75, 100 and 400 m depth. Figure 4-7 shows the finite difference mesh of the model. The blue lines indicate the fractures.

Table 4-2. Case/problem overview.

Case/Tunnel spacing		Repository	Principal stress case	Direction α
Case 1	Without (base case)	No	σ_1=50 MPa, σ_2=10 MPa	30°
	40 m (base case)	Yes		
	30 m			
	20 m			
	15 m			
	10 m			
Case 2	Without (base case)	No		10°
	40 m (base case)	Yes		
	30 m			
	20 m			
	15 m			
	10 m			
Case 3	Without (base case)	No	σ_1=70 MPa, σ_2=10 MPa	27.5°
	40 m (base case)	Yes		
	30 m			
	20 m			
	15 m			
	10 m			
Case 4	Without (base case)	No		45°
	40 m (base case)	Yes		
	30 m			
	20 m			
	15 m			
	10 m			

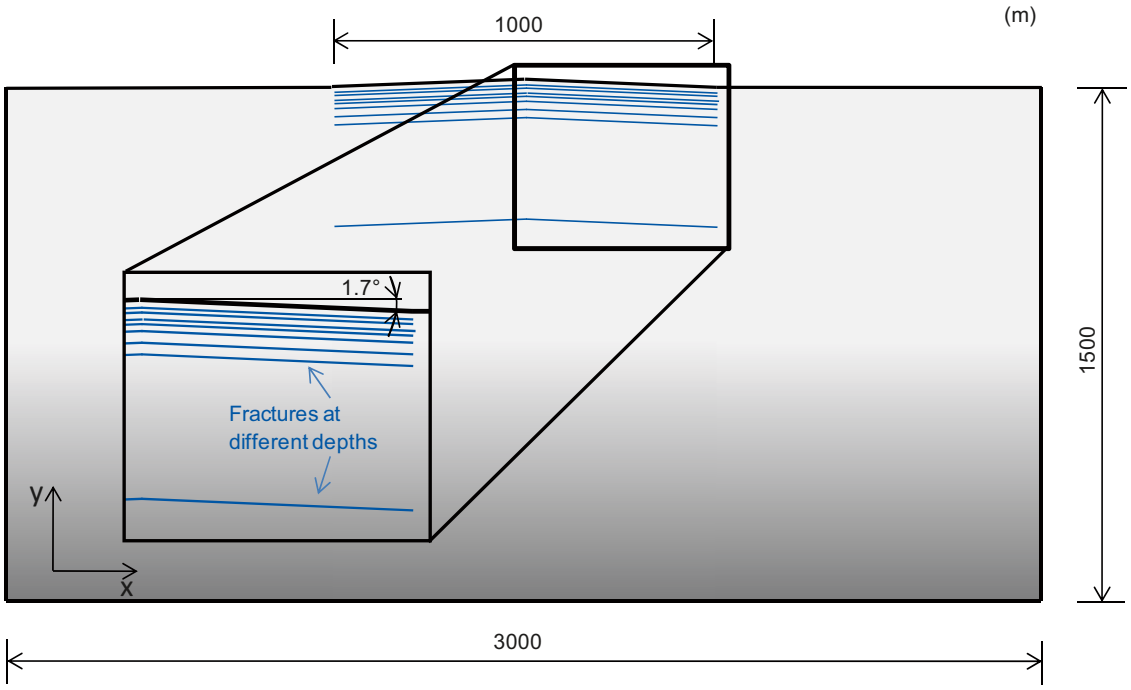

Figure 4-6. *Outline and dimensions of the sheeting model. Fractures (blue) are included at 10, 20, 30, 40, 50, 75, 100 and 400 m depth. The upper boundary represents the ground surface. The mid-point of the upper boundary is shifted 15 m in the positive y-direction in order to resemble a curved ground surface above the fractures. The fractures have the same shape as the inclined ground surface above them, i.e. inclined about 1.7° outward in both the positive and negative x-directions.*

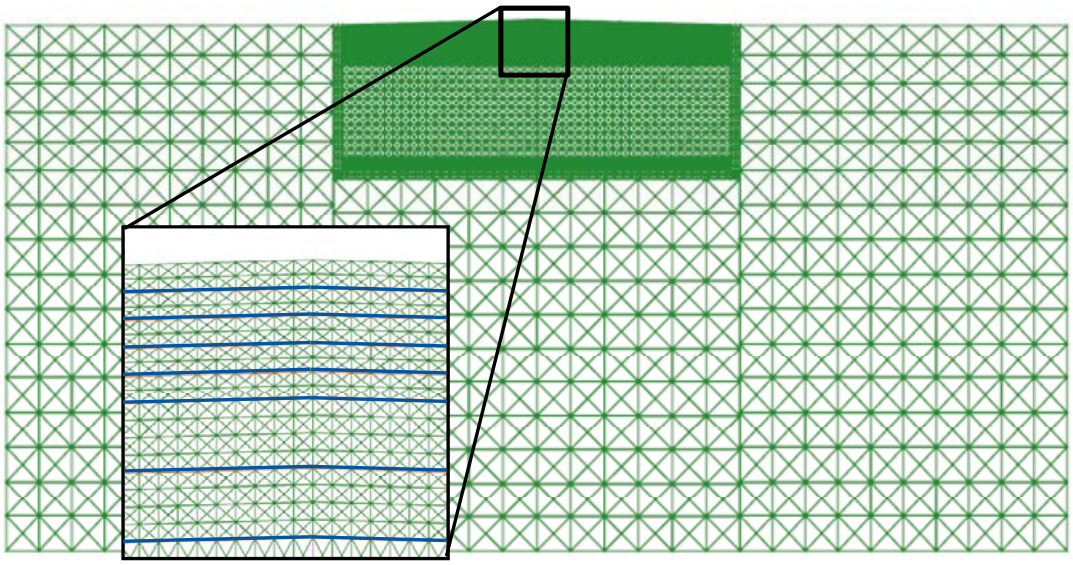

Figure 4-7. *The finite difference mesh of the model. The fractures are indicated by the blue lines.*

4.3.2 Constitutive models

The constitutive models for both the continuum and the fractures are described in Section 4.2.2. The parameter values are set according to Table 4-3. The values for the fractures are in accordance with site investigation data /Glamheden et al. 2007/.

4.3.3 Analysis steps, initial conditions and boundary conditions

The analysis comprises the following steps (Figure 4-8):

1. Initial equilibrium: Initial stresses are applied (Table 4-4) and initial equilibrium is achieved under gravity. Both the vertical boundaries and the bottom boundary are locked for normal displacements.
2. Compression: The vertical boundaries are moved towards the model centre. The resulting displacements correspond to a nominal σ_{xx}-increase of 40 MPa. The bottom boundary is locked for normal displacements.
3. Final equilibrium: The model is allowed to achieve equilibrium. Both the vertical boundaries and the bottom boundary are locked for normal displacements.

The σ_{xx}- and σ_{yy}-initial stress components (Table 4-4) are in accordance with the *in situ* stress estimates for the Forsmark site /Glamheden et al. 2007/. The effect of a hydrostatic pore water pressure is applied in the fractures during all analysis steps.

Table 4-3. Material property parameter values.

	Parameter	Value	Unit
Continuum	Young's modulus, E	68	GPa
	Poisson's ratio, υ	0.22	–
	Density, ρ	2,700	kg/m^3
Fractures	Normal stiffness, k_n	500	GPa/m
	Shear stiffness, k_s	30	GPa/m
	Friction angle, φ	35	deg
	Cohesion, c	0.5	MPa
	Tensile strength, σ_n^*	0	MPa

Table 4-4. Initial stresses. Compressive stresses are positive and *y* is zero at the ground surface and negative below. The σ_{zz}-component is in the out-of-plane direction. The σ_{xx}- and σ_{yy}-components are in accordance with the *in situ* stress estimates for the Forsmark site /Glamheden et al. 2007/.

Component	Depth variation
σ_{xx}	10–0.075*y*
σ_{yy}	–0.0265*y*
σ_{zz}	10–0.035*y*
σ_{xy}	0

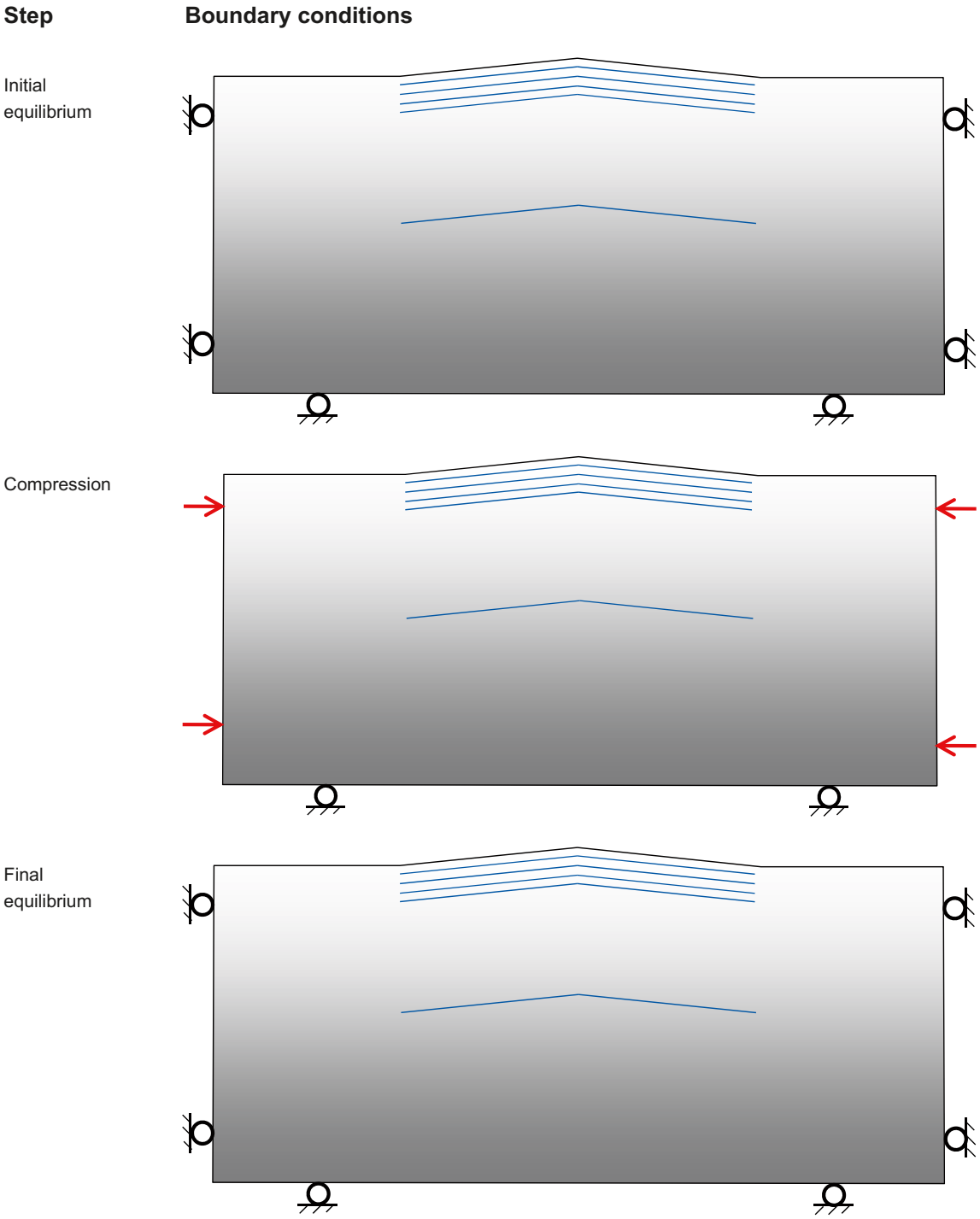

Figure 4-8. *Analysis steps and corresponding boundary conditions.*

5 Modelling results

5.1 Shearing model

This section presents model results from the shear load model. Results for the case without tunnels are presented along with the case with tunnels. Several diagrams show results from the centre of the fracture (e.g. the nearest grid point to the centre, about 0.5 m offset). This recording point is located as shown in Figure 5-1.

The 40 m tunnel spacing assumption is a base case and most of the results shown here regard this case. Other tunnel spacings have also been tested. Results from these cases are summarised in bar graphs. The stress results are also used as input to the stability evaluation in Chapter 6.

5.1.1 Shear- and normal stresses

The transition from initial state to the state after slip is presented in Figure 5-2 (shear and normal stress) as functions of the prescribed cohesion. The results are evaluated at the centre of the fracture. The following can be observed:

- Without tunnels: The stress drop obtained at the onset of failure is equal to the applied cohesion, c. This is because of the displacement-weakening material law which means that the cohesion is set to zero as the shear strength is exceeded (cf. Section 4.2.2). For all subsequent analysis steps, the shear strength depends on the normal stress only, i.e. $\tau = \tan(\varphi)\sigma_n$.
- With tunnels: Both normal- and shear stresses are higher than in the case without tunnels. The openings result in higher stresses in the rock volumes between them. It can also be observed that the stress drop obtained at shear failure is unequal to the applied cohesion. This is due to the uneven distribution of shear stress along the fracture; the applied cohesion has to be high enough to prevent failure at the locations where the stability is as lowest (due to low normal stress combined with high shear stress). These parts will be the first to slip. As slip is initiated at these locations, the stresses are redistributed such that the remaining parts of the fracture fail.

Figure 5-3 and Figure 5-4 show the variation along the fracture before and after slip for shear and normal stresses, respectively. In the models without tunnels, the change in shear stress due to slip is in accordance with Figure 5-2, whereas there is no change in normal stress.

In the models with tunnels, there is a variation in both shear and normal stresses along the fracture. In general, the stresses are higher close to the tunnel openings. It should be noted that since the tunnels are here schematically modelled as square shaped openings, the model cannot be used for a detailed study of the stress situation around tunnel openings. Similar to the case without tunnels, the shear stresses are in general reduced at slip whereas the normal stresses stays effectively unchanged.

The initial shear- and normal stresses along the fracture are used as input to the stability evaluation in Chapter 6, where the stability is evaluated for different tunnel spacings.

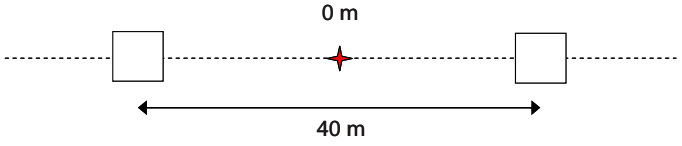

Figure 5-1. *Location of history point at the centre of the fracture (0 m).The tunnel spacing is 40 m.*

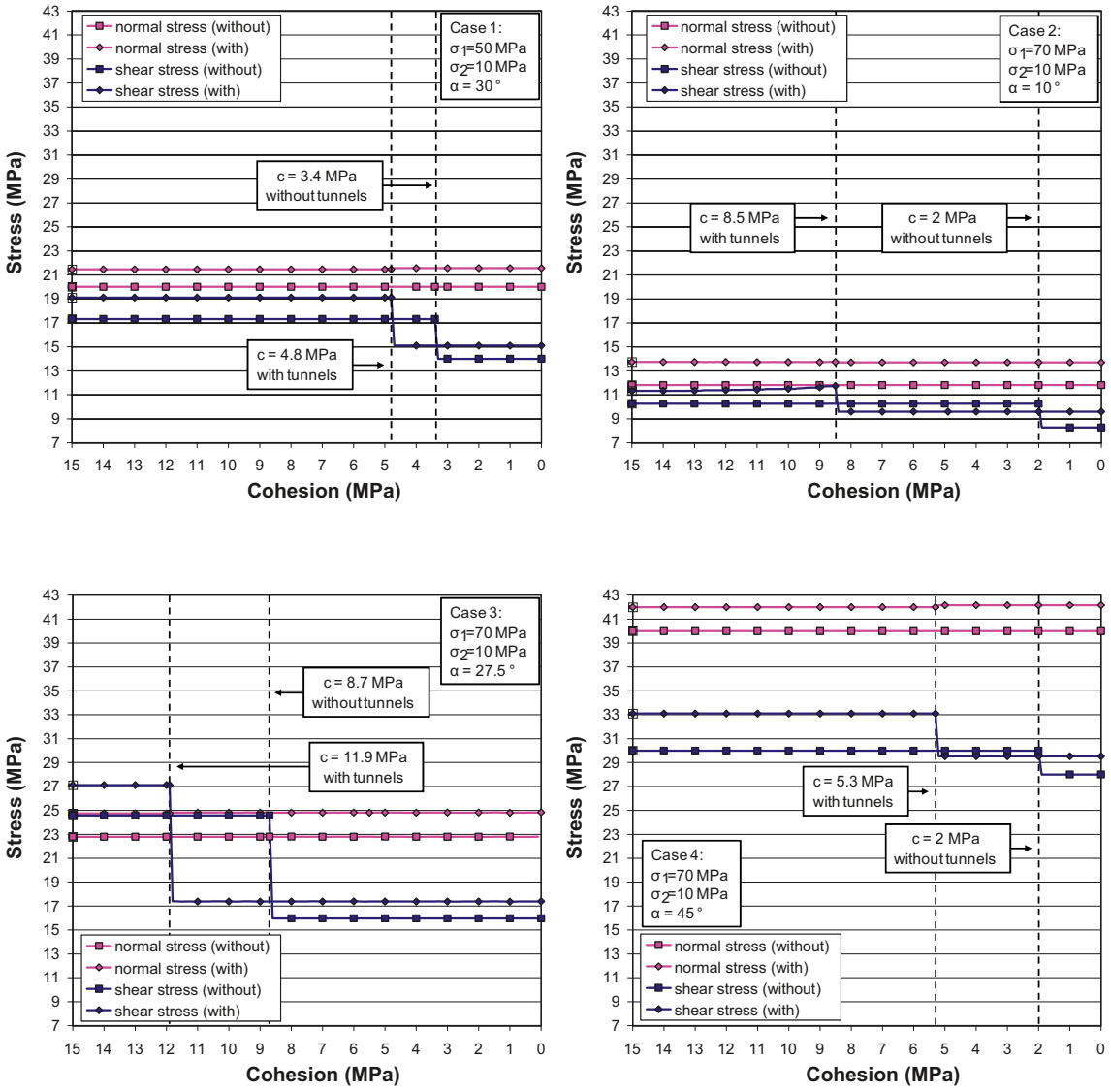

Figure 5-2. *Shear stress and normal stress at the centre of the fracture in all four stress cases. The curves show the transition from the initial state to the state after slip. Note that, for the models without tunnels, the stress drop is equal to the applied cohesion.*

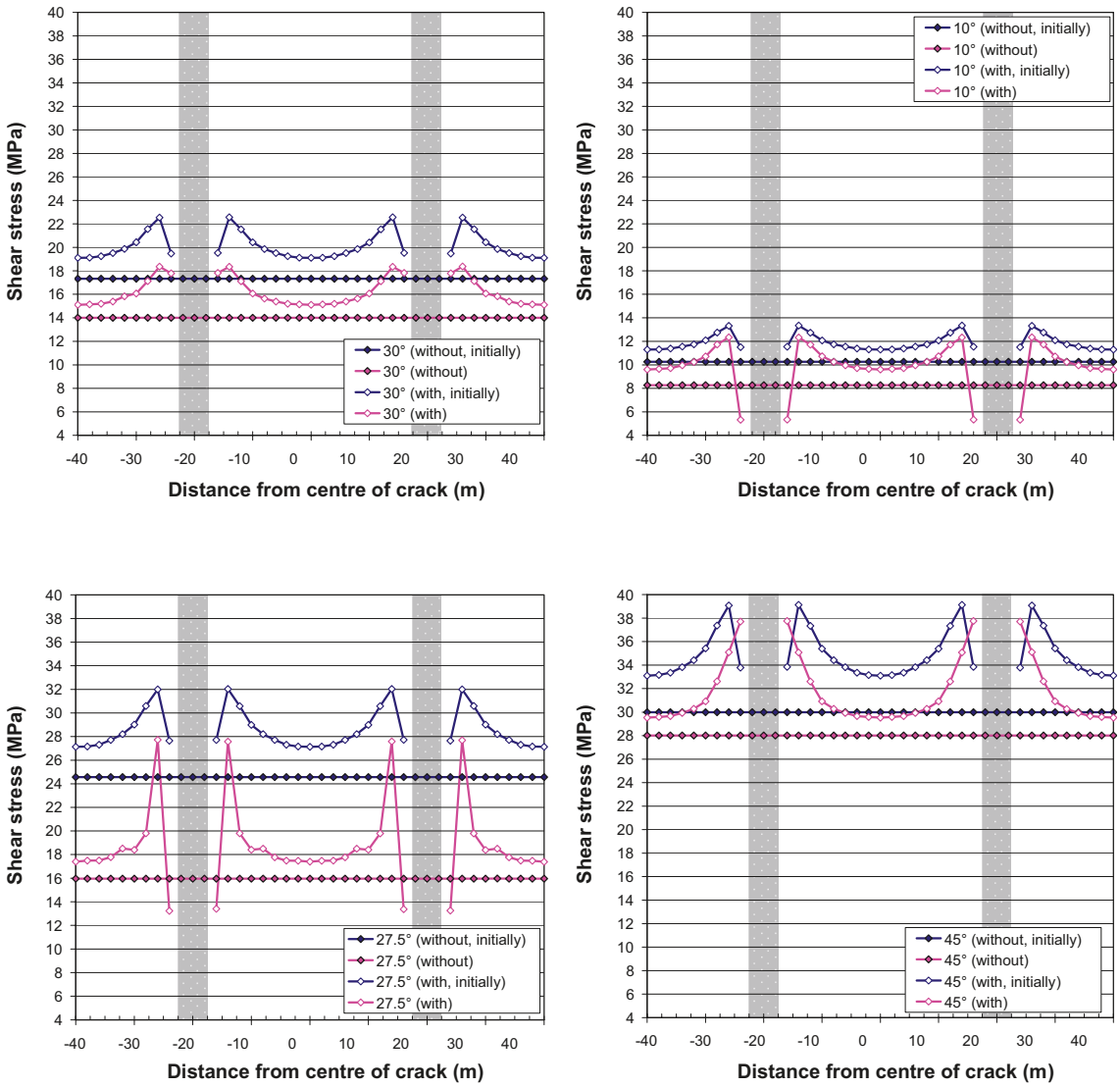

Figure 5-3. *Shear stress before and after slip for models with and without tunnels. Grey areas represent tunnel interior.*

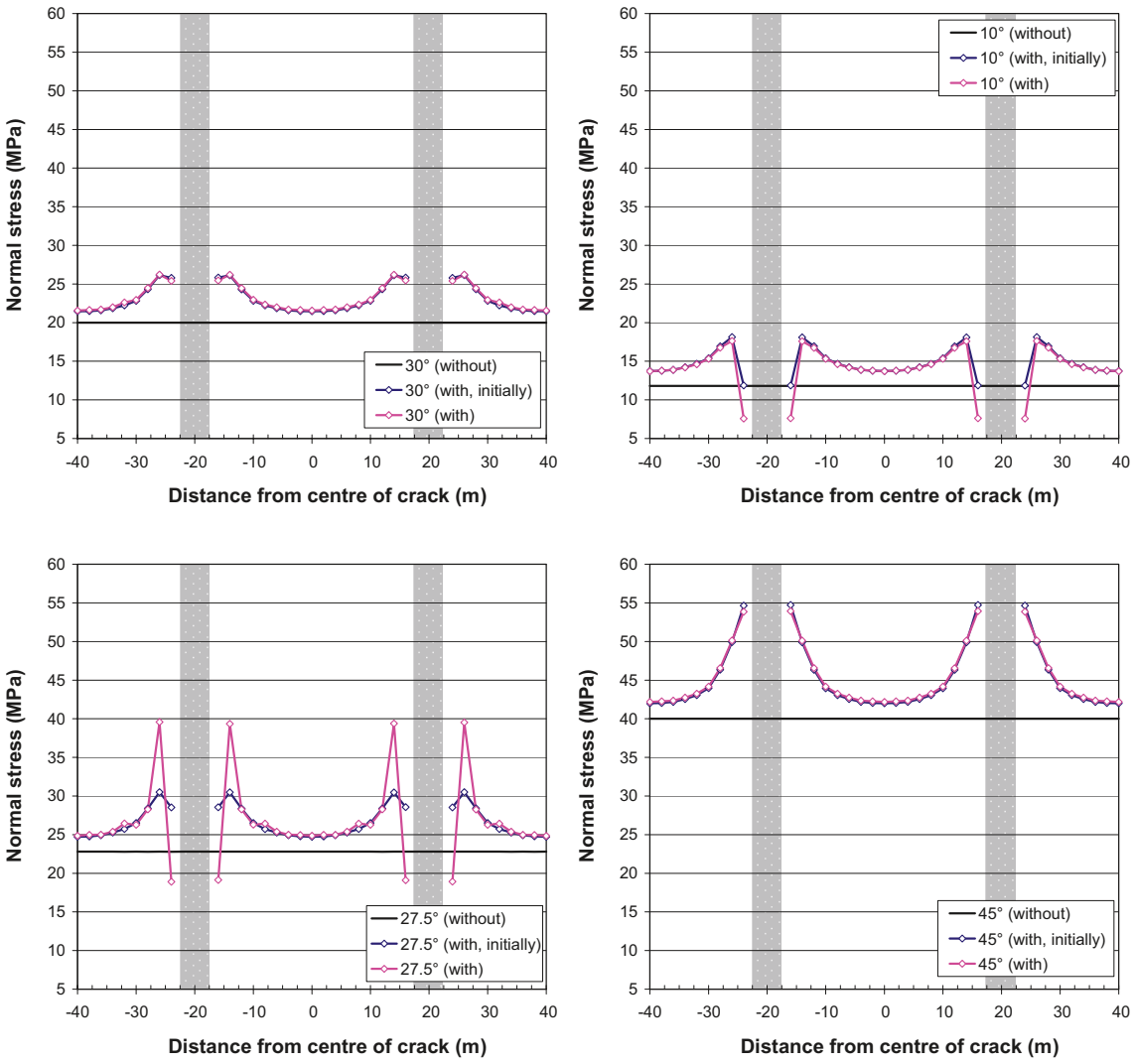

Figure 5-4. *Normal stress before and after slip for models with and without tunnels. Grey areas represent tunnel interior.*

Figure 5-5 shows the shear and normal stresses at the centre of the fracture initially and after slip for each of the four stress states and for different values of the tunnel spacing. The following can be observed:

- Introducing a system of tunnels separated by 40 m to the rock will increase the initial shear stress by about 10%. The corresponding increase in shear stress due to tunnel spacings of 30 m, 20 m, 15 m and 10 m are around 20%, 40%, 70% and 160%, respectively. There is very little variation between the stress states.
- There is some increase of the normal stress due to the presence of tunnels. The increase in initial normal stress is 1.5–2 MPa, 2.7–3.7 MPa and 6–8.7 MPa for 40 m, 30 m and 20 m tunnel spacing, respectively. For tunnel spacings less than 20 m there are larger variations in the increase of normal stress between the different stress states.
- The shear stresses are reduced as the fracture slips. The stress reductions are different for different tunnel spacings and different stress states. The maximum relative shear stress reduction is about 35%.
- Except for the model with 10 m tunnel spacing, there are only minor changes in normal stress due to fracture slip. In the model without tunnels, the normal stress is not changed.

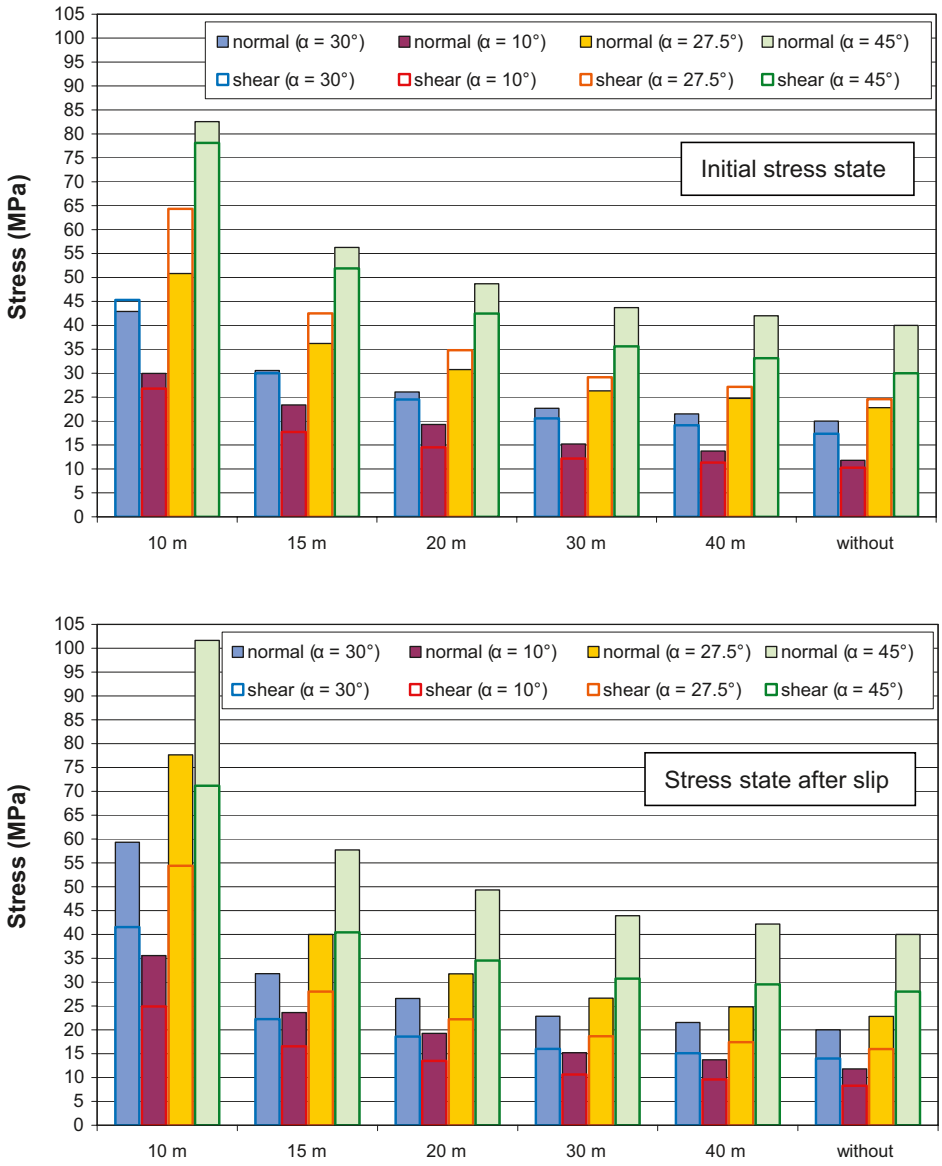

Figure 5-5. *Initial shear- and normal stresses (top) and shear- and normal stresses after slip (bottom) for given stress states and tunnel spacings. The results are picked at the centre of the fracture.*

5.1.2 Shear displacements

The total shear displacement at the centre of the fracture is not significantly affected by the presence of the repository, cf. Figure 5-6. For the cases considered here, the total shear displacement at the centre of the fracture is increased up to approximately 1.6% (Case 3) when the repository is included in the model. For the other three cases, the shear displacement increases by less than 1% when the tunnels are included in the model.

Figure 5-7 shows the variation in shear displacement along the fracture over a distance corresponding to two tunnel spacings. The positions of the tunnels are marked in grey. In each of the figures, the variation along the entire fracture is shown as an inset. As seen in the insets, the displacements reach their largest values at the centre of the fracture. As noted above, the displacements are effectively unchanged due to the presence of the tunnels.

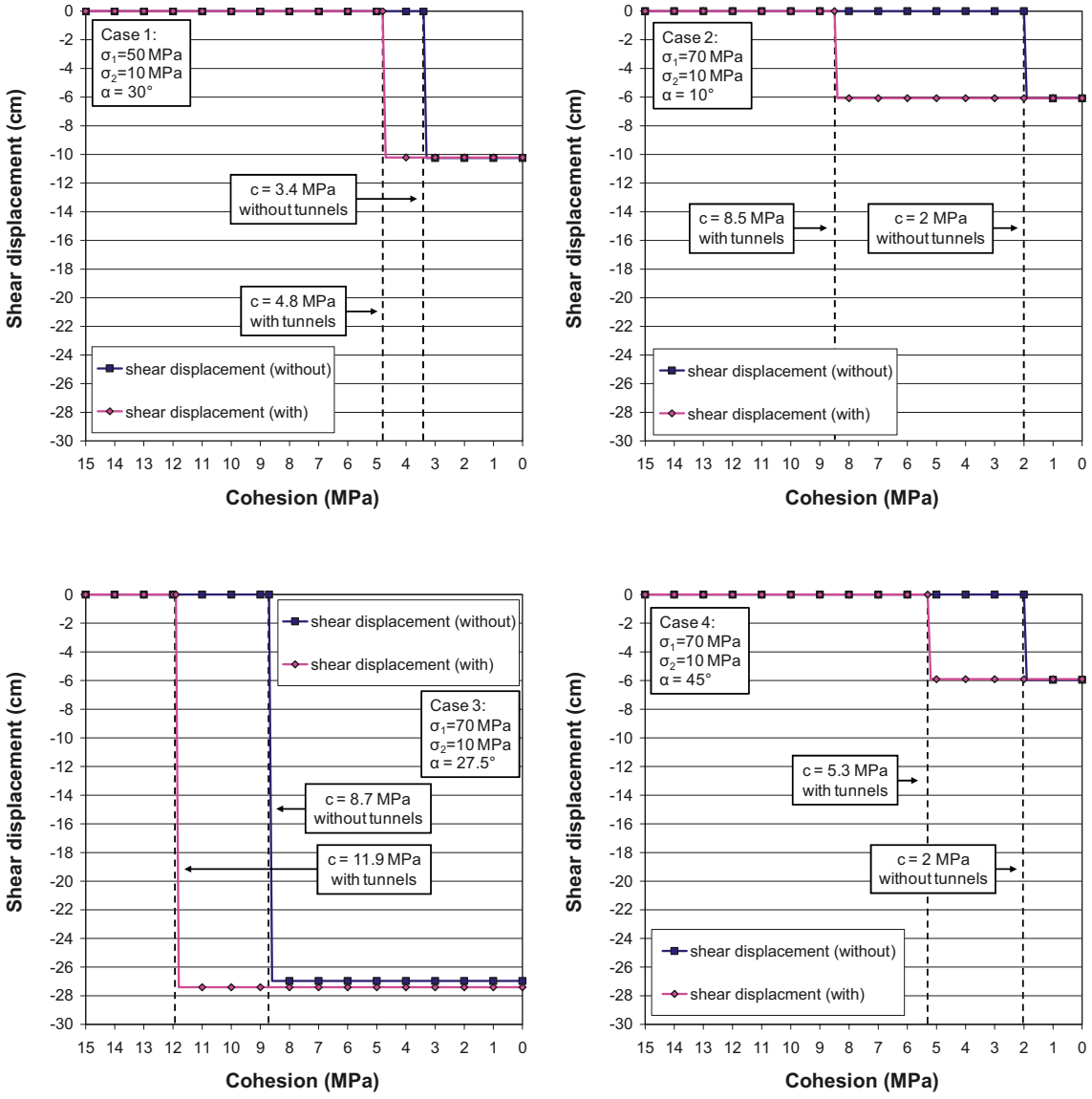

Figure 5-6. *Shear displacement at the centre of the fracture in all four stress cases. The curves show the transition from the initial state to the state after slip.*

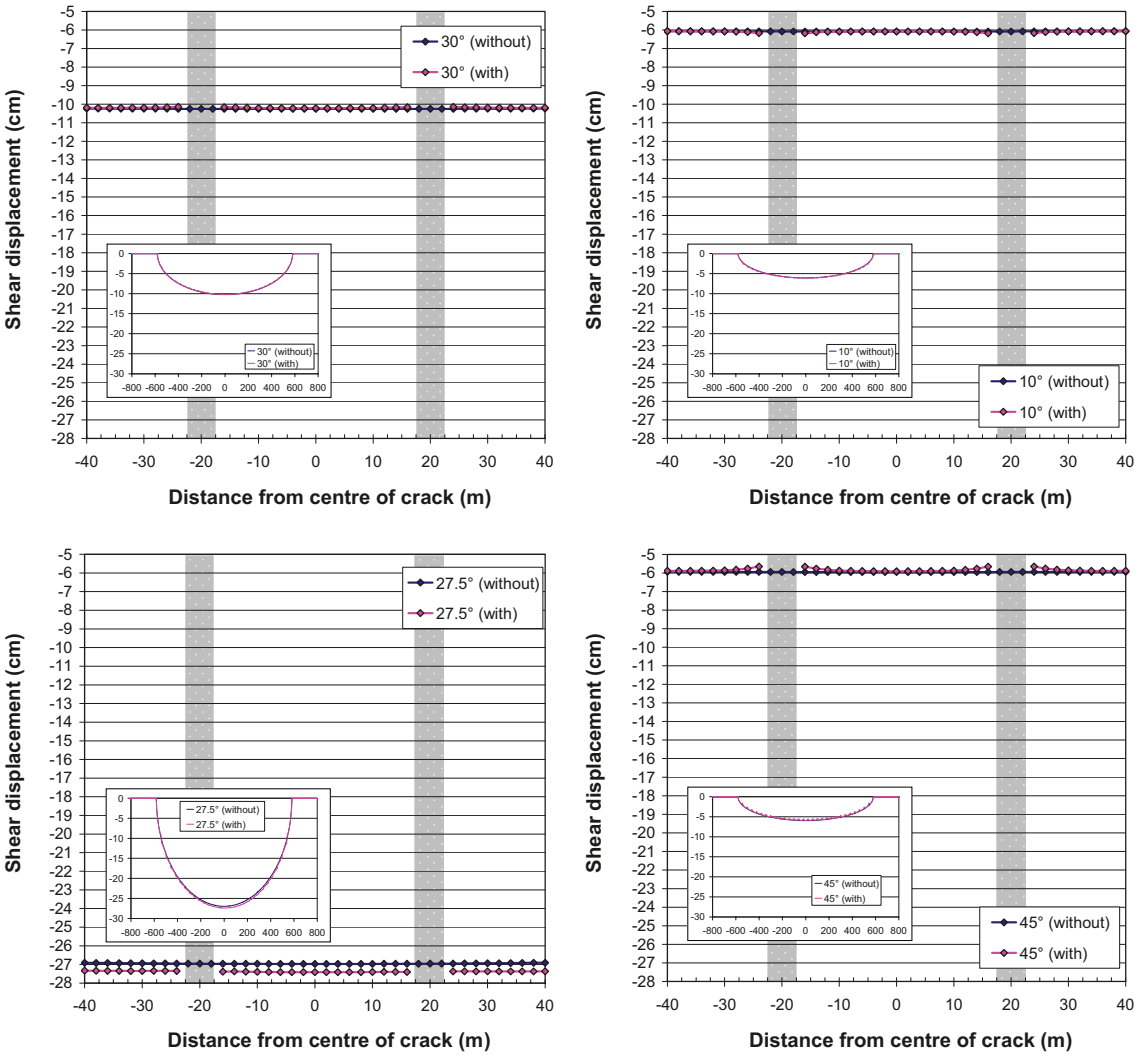

Figure 5-7. *Shear displacement for models with and without tunnels. Inset shows the displacement along the entire fracture. Grey areas represent tunnel interior.*

Figure 5-8 shows the shear displacement at the centre of the fracture for different values of the tunnel spacing. As seen in the figure, reducing the tunnel spacing does not seem to have any significant impact on the displacements. This is a natural consequence of the constitutive law for the fracture; failure results in frictional only behaviour following failure. This means that the fracture behaviour after failure is independent of the contact area, but merely on the friction coefficient, which is the same for all models.

It can be noted that in stress Case 3 ($\alpha = 27.5°$), the displacements are significantly larger compared to the other cases. This is caused by the larger stress drop (reduction of shear stress) at slip obtained with this stress model (cf. Figure 5-2 and Figure 5-3). The stress drop is governed by the stress state (stress and anisotropy stress orientation), and in the 27.5°-case, the stresses are oriented in order to give largest possible stress drop at the given stress magnitudes.

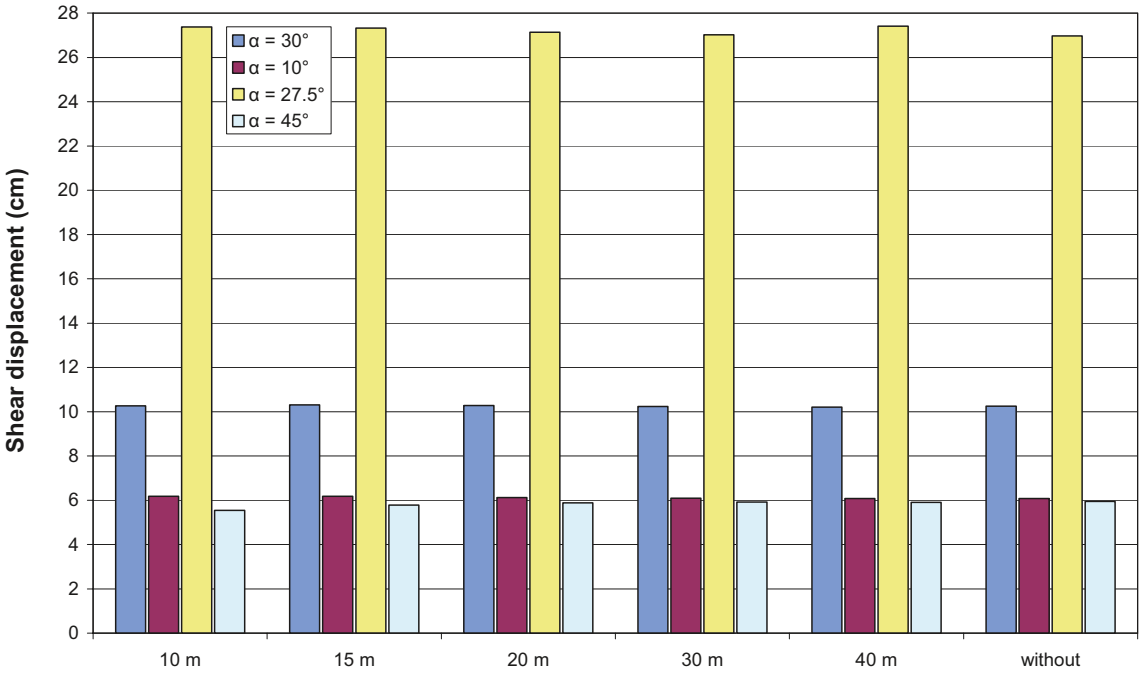

Figure 5-8. *Shear displacement at the centre of the fracture at given tunnel spacing compared with a corresponding case without tunnels. It can be noted that stress Case 3 (α = 27.5°), the displacements are significantly larger compared to the other cases. This is caused by the larger stress drop (reduction of shear stress) at slip obtained with this stress model.*

5.2 Sheeting model

This section presents the results from the sheeting analysis. Figure 5-9 shows the resulting displacements at the end of the analysis when the model has been compressed in the horizontal direction. The vector lengths are scaled according to their magnitudes. Note how the upper boundary is lifted due to the compression. The vertical displacements of the boundary are emphasized just above the central part of the model (see inset). This is caused by opening (sheeting) of the fractures close to the upper boundary.

The compression of the model causes a large horizontal stress increase. The displacements at the vertical boundaries are calibrated to give a nominal horizontal (σ_{xx}) stress increase of about 40 MPa. The temporal evolutions of σ_{xx}-stresses at three recording points (26 m, 53 m and 500 m depth) are shown in Figure 5-10. The horizontal stress increase at 500 m depth is in accordance with the nominal calibrated value (left). At the shallow depths, however, the increase is lower. This is due to the opening of the fractures close to the ground surface with corresponding larger heave of the ground surface as a consequence. This results in stress relaxations.

The evolutions of σ_{yy}-stresses are shown in the lower right graph of Figure 5-10. There is a sudden jump in the stress at 53 m depth. This is related to the opening of fractures at shallow depths. The resulting σ_{yy}-stress change at 500 m depth is moderate, about 0.5 MPa.

Figure 5-11 shows the evolution of the effective normal stresses in the middle of the fractures. The normal stresses are plotted versus the σ_{xx}-stress increase at 500 m depth (cf. Figure 5-10, lower left). Zero effective normal stress indicates that a fracture has been opened, i.e. that sheeting has occurred. The horizontal stress increase needed to open up a fracture depends on the depth of the fracture. The fracture at 10 m depth is opened at a σ_{xx}-stress increase of about 3 MPa, whereas the stress increase is about 7.5 MPa when the fractures at 20 – 50 m depths are opened. The fractures at 75 m and 100 m depths are opened at 13.5 MPa and 22 MPa stress increase, respectively. At 400 m depth, the resulting normal stress reduction is about 0.5 MPa and the fracture is far from being opened.

Figure 5-12 shows a plot at the end state of the analysis. The black lines indicate parts of the fractures with zero normal stress. The picture shows how only the central parts of the fractures have been opened. It also shows that the extent of sheeting is larger at more shallow depths.

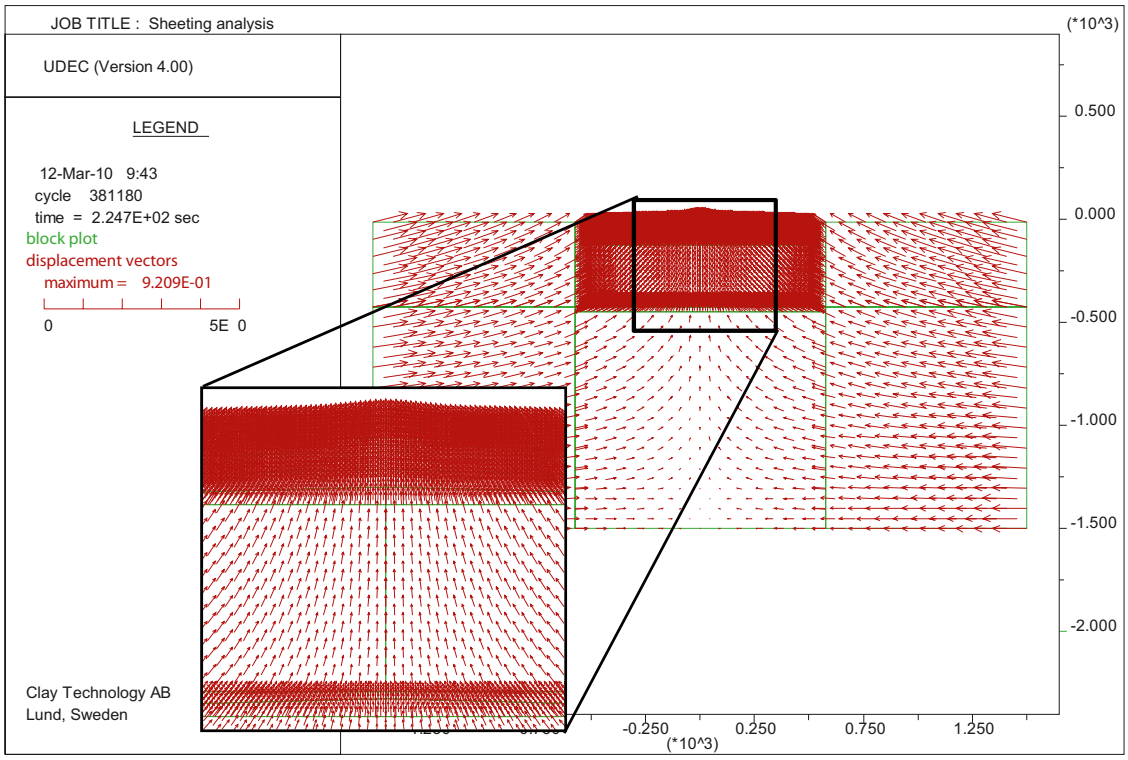

Figure 5-9. *Displacement vectors at the end of the analysis. Note the larger vertical displacements close to the upper boundary in the central part of the model.*

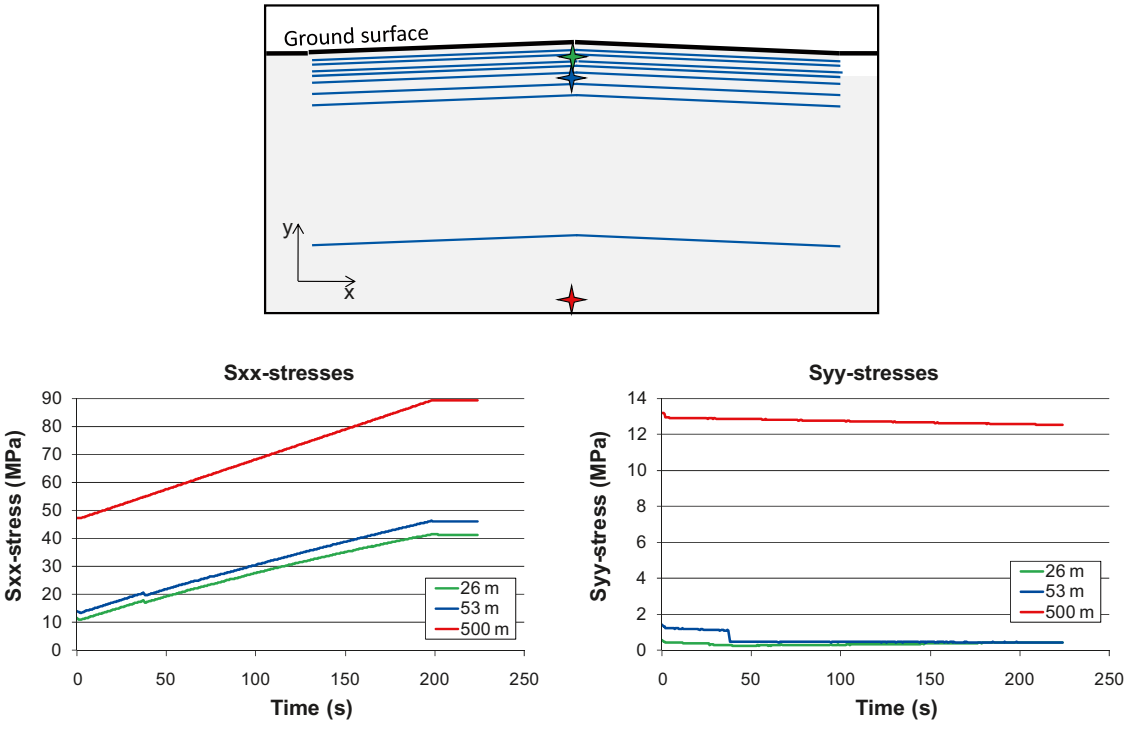

Figure 5-10. *Upper: Sketch showing locations of recording points for stresses. Lower: σ_{xx}-stresses (left) and σ_{yy}-stresses (right) at three different depths (26 m, 53 m 500 m). The σ_{xx}-stress at 500 m depth is increased about 40 MPa due to the compression of the model. Note that the time given by the x-axes not is physical time, but only model time used in the quasi-static model.*

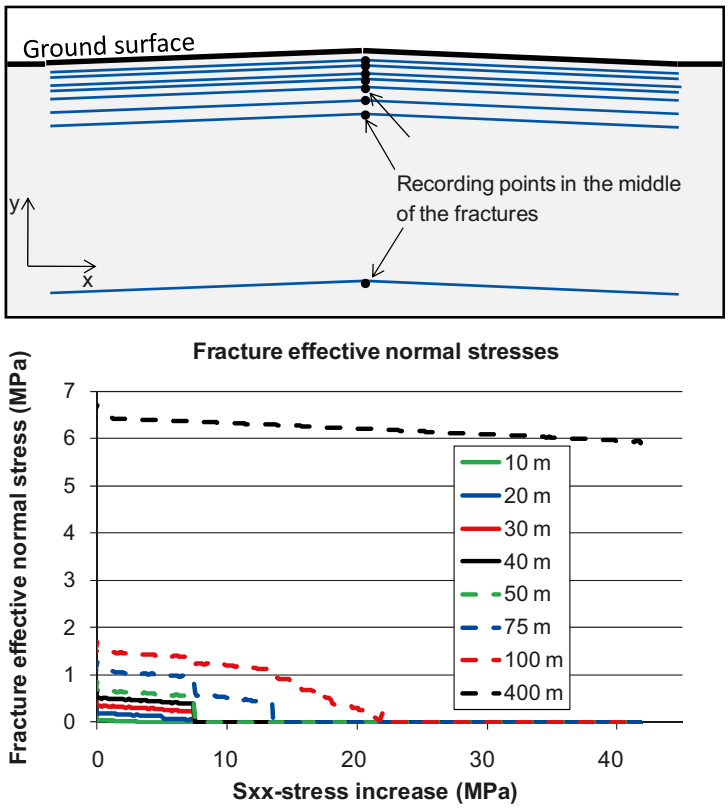

Figure 5-11. *Upper: Sketch showing locations of recording points for fracture normal stresses. Lower: Fracture effective normal stresses at given depths recorded in the middle of the fractures. The normal stresses are plotted versus the σ_{xx}-stress increase at 500 m depth (cf. Figure 5-10, lower left).*

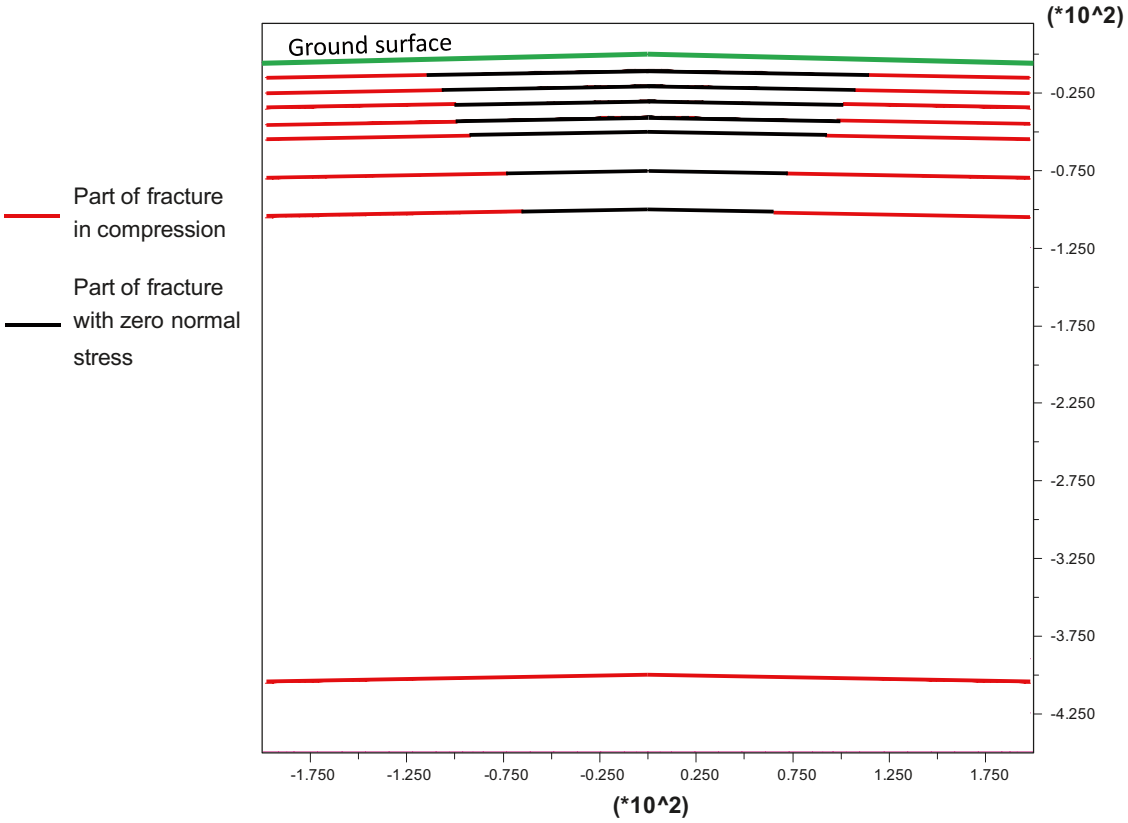

Figure 5-12. *Status at the end of the analysis. The picture shows how only the central parts of the fractures have opened up.*

6 Evaluation of stability

In order to assess the repository as a plane of weakness, the stability of the fracture intersecting the tunnel openings in the shearing model is evaluated. The stability is evaluated also for the sheeting case.

6.1 Shearing

The stability is evaluated using input from two sources:

Stresses from the static shear load models analysed in this study (cf. Section 5.1.1). The normal- and shear stresses in the initial state (before slip) are used.

Stresses from dynamic earthquake simulations /Fälth et al. 2010/. Normal- and shear stresses in horizontal fracture planes at two different locations relative a rupturing fault are used to evaluate the stability of the rock mass.

6.1.1 Using input from static models

The stability of the fracture is evaluated using the parameter FoS (Factor of Safety). FoS is defined as the ratio between the shear strength and the shear stress, i.e.

$$FoS = \frac{(\sigma_n - P)\tan\varphi + c}{\tau} \qquad \textit{Equation 6-1}$$

where σ_n is the normal stress, P the pore pressure, φ is the friction angle, c is the cohesion and τ is the shear stress acting in the plane. As can be seen, FoS = 1 means that the fracture is at the limit of failure. FoS > 1 means stability.

The FoS is calculated along the fracture plane in a gap between two tunnels. The values of friction angle, φ, and cohesion, c, are assumed to be in accordance with the values estimated for the rock mass at the Forsmark site /Glamheden et al. 2007/, i.e. $\varphi = 50°$ and $c = 20$ MPa.

The pore pressure, P, is set at 6 MPa. This is based on the assumption that the stability is evaluated for an end-glacial situation and that there is a glacially-induced 1 MPa excess pore pressure at repository depth. This is in accordance with estimates by /Hökmark et al. 2010/.

The calculation is done for all four stress states and for all tunnel spacings (40 m, 30 m, 20 m, 15 m and 10 m). The results are presented in Figure 6-1. The following can be observed:

- The results indicate that the sensitivity of the stability margin to the presence of tunnels is modest. Including tunnels with 40 m spacing gives a reduction of the stability margin by about 20% at a maximum.
- The results suggest that the tunnel spacing can be reduced to about 20 m without any risk of failure. In the 27.5° stress state, which is designed to give maximum instability, FoS is higher than 1.4 for all tunnel spacings larger than 20 m (lower left).

The limited sensitivity to the presence of the tunnels is caused by the fact that the shear stress increase caused by the tunnels is accompanied by a corresponding normal stress increase. The increase of normal stress results in a higher shear strength that balances the higher shear stress. As have been noted earlier, the hypothetical stress states used here give high shear loads which thus result in low Factor of Safety values.

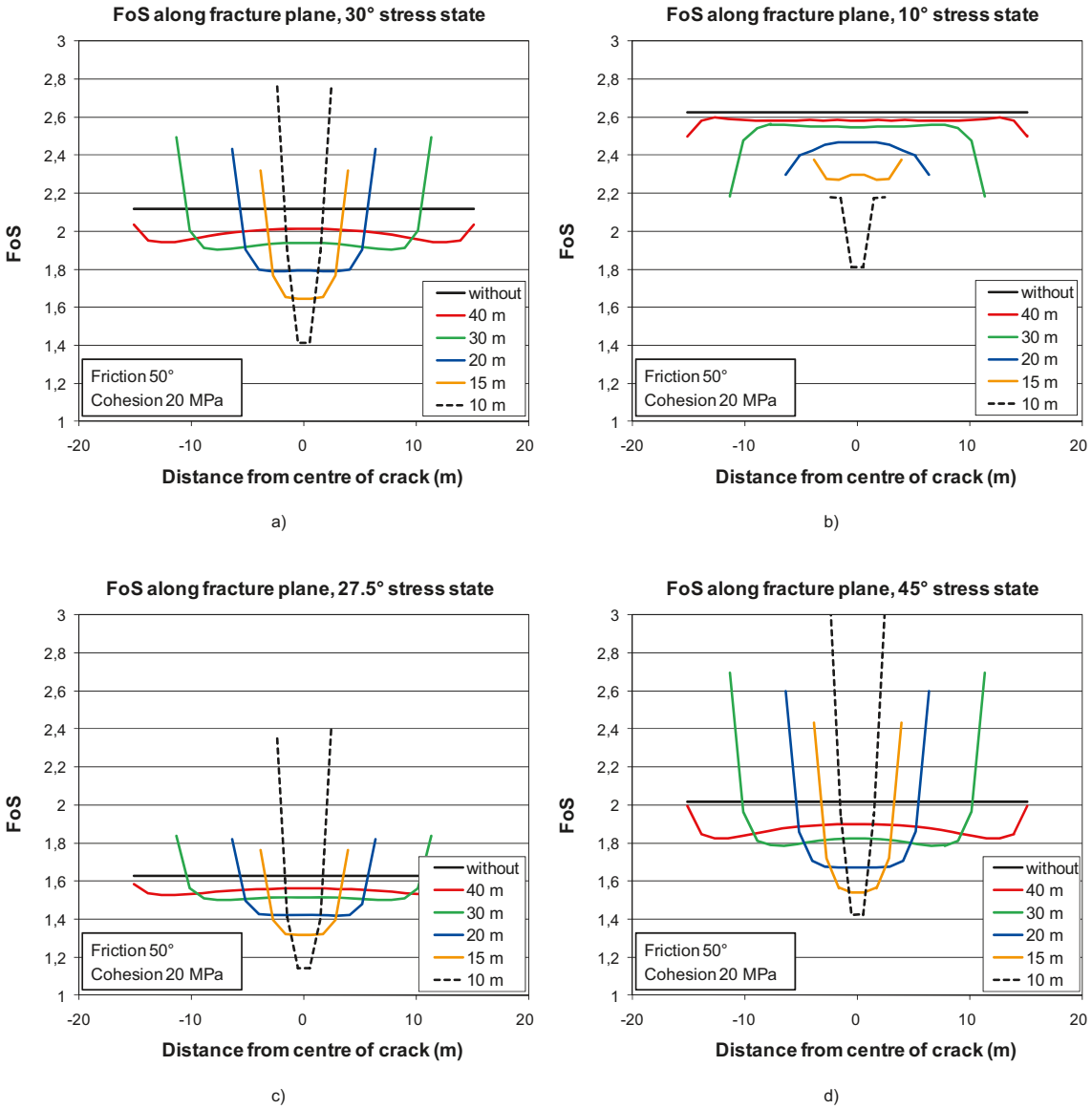

Figure 6-1. *FoS along the fracture plane between two tunnels. The results indicate that the stability of the fracture has a low sensitivity to the presence of the tunnels. FoS is higher than 1.4 for all tunnel spacings larger than 20 m.*

6.1.2 Using input from dynamic earthquake simulations

During an earthquake, the slipping fault produces stress waves that will have an impact on the surrounding rock mass. The potential impact of an earthquake on the KBS-3 repository in terms of induced rock fracture shear displacements has been studied by /Fälth et al. 2010/. They did this by running generic dynamic earthquake simulations. In addition to shear displacements in fractures, the temporal development of normal- and shear stresses in a number of differently oriented planes at different locations relative to the rupturing fault were recorded. This provided the possibility to study the potential stability development at these locations.

Figure 6-2 shows the temporal development of normal-and shear stresses in horizontal planes at 500 m depth at two locations relative to the rupturing fault in a model simulating a M_w 6.2 earthquake /Fälth et al. 2010/. At both locations, the stresses are monitored at a distance of 200 m from the fault plane. The left diagram shows stresses recorded far from the fault's vertical edge and the right diagram the stresses close to the fault edge. The locations are indicated by the insets. The stresses at $t = 0$ correspond to the initial state, i.e. before the earthquake. At this time the shear stress is almost zero and the normal stress is relatively high. This gives a high initial stability. At the point far from the fault edge (a) the

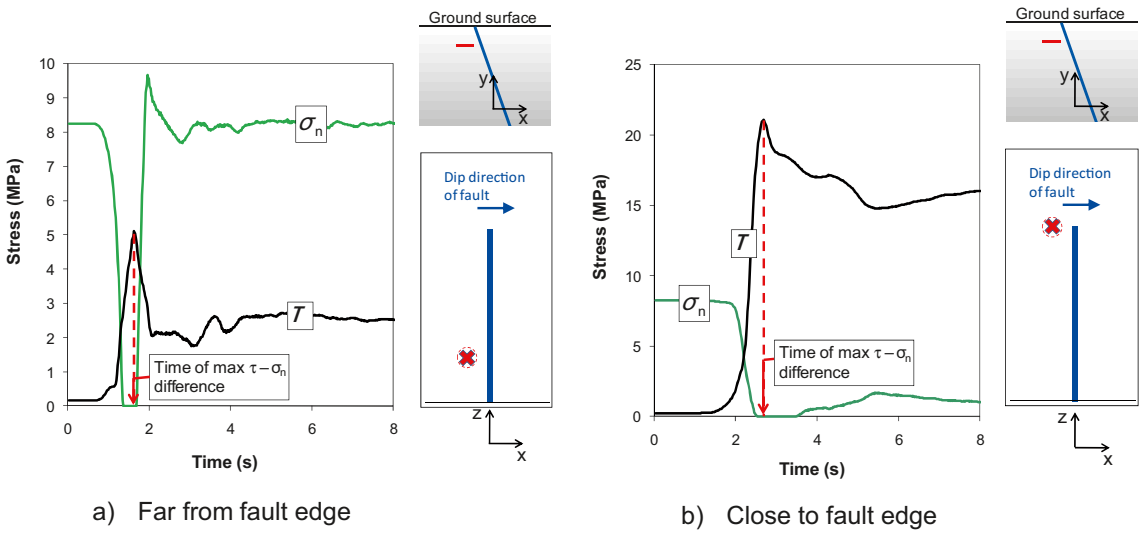

Figure 6-2. *Results from dynamic earthquake simulation of a M_w 6.2 earthquake /Fälth et al. 2010/. Temporal development of normal- and shear stresses in horizontal planes located (a) far from fault edge and (b) close to fault edge. The locations of the recording points are indicated by the insets to the right of each diagram. The time of maximum difference between shear- and normal stress is indicated by the red dashed lines.*

dynamic pulse causes a sudden increase of the shear stress, τ, and a simultaneous reduction of the normal stress, σ_n, down to zero. The shear stress is higher than the normal stress during about 0.5 s. Close to the fault edge (b), the stress redistributions results in shear stress increase and normal stress decrease such that the shear stress remains considerably higher than the normal stress after the earthquake.

The time of maximum difference between shear- and normal stress, and thus a corresponding maximum instability, is indicated by the red dashed lines. The stresses at these time instances are used in the stability evaluation below.

The stresses at the time of maximum τ - σ_n difference indicated in Figure 6-2 are used to calculate the Factor of Safety (FoS) for the case without tunnels and for different tunnel spacings. In order to account for different tunnel spacings, Equation is rewritten:

$$FoS = \frac{((\sigma_n/h) - P)\tan\varphi + c}{\tau/h}$$

Equation 6-2

$$h = 1 - \frac{t}{s} \qquad s > t$$

where t is the tunnel width set to 5 m and s is the tunnel spacing. By setting s to a large value, the FoS for the case without tunnels is obtained. This way of accounting for the tunnels means that the FoS calculated here is and average value for the rock mass between the tunnels. The assumed parameter values of friction angle and cohesion are the same as in Section 6.1.1, i.e. φ = 50° and c = 20 MPa. The results are plotted in Figure 6-3. The following can be observed:

- Far from the fault edge, there is a high stability (FoS=4) without tunnels. Introducing the tunnels gives a FoS reduction to 3.5. As the tunnel spacing is reduced, the shear loads are distributed over smaller areas and the safety margin is reduced, but even with 10 m spacing the FoS is as high as 2.
- Close to the fault edge the rock is at the stability limit without tunnels. The low stability is caused by the large shear stress combined with zero normal stress (cf. Figure 6-2b). Introducing a system of tunnels with 40 m spacing gives a slight FoS reduction, i.e. the rock is taken into a state of failure.

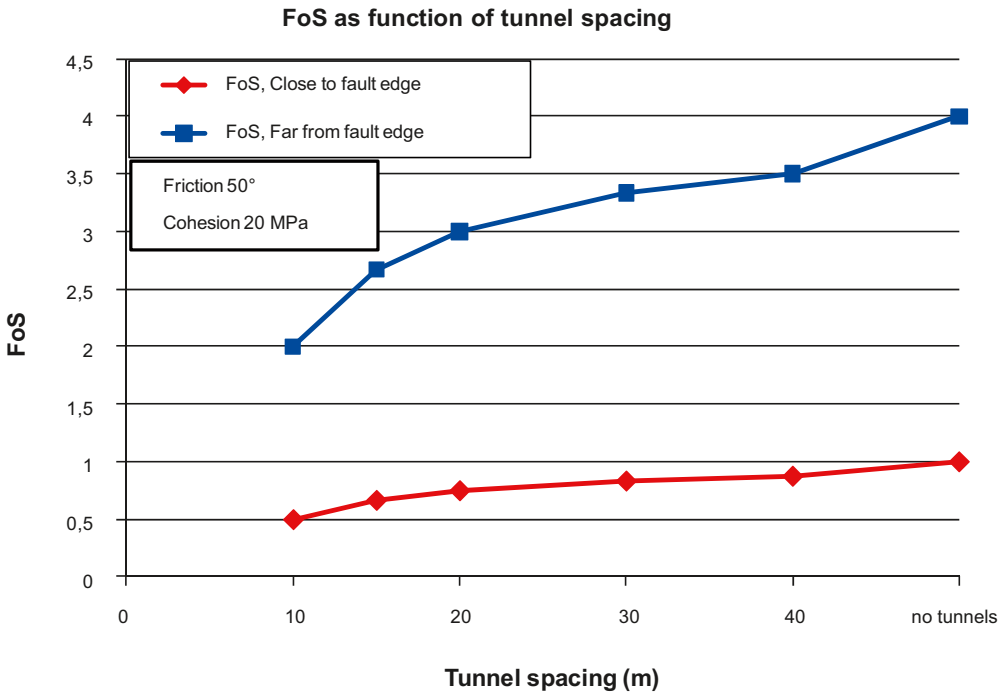

Figure 6-3. *FoS as function of tunnel spacing at two different locations around a rupturing earthquake fault. The FoS values are based on normal- and shear stresses in horizontal planes at 500 m depth. The stresses are obtained from dynamic earthquake simulations by /Fälth et al. 2010/.*

6.2 Sheeting

According to the sheeting simulation (Section 5.2) the normal stress at 400 m depth is reduced from 6.5 MPa to 6 MPa, i.e. a minor reduction of about 8% when the horizontal stress is increased by 40 MPa. The fracture at 400 m depth has the same inclination (about 1.7°) as the fractures at shallow depths. In the projected repository, the tunnels will be inclined 1:100 (about 0.6°) for drainage purposes /SKB 2009b, SKB 2010b/. This inclination is about 1/3 of that applied in the models here. Thus, in this respect, the normal stress reduction recorded at 400 m depth in the model is an overestimate rather than an underestimate.

The model does not include any tunnel openings. However, at locations where the rock is compressed and there is no tendency to open up the fracture, adding a system of tunnels does not reduce this compression and therefore will not increase the risk of sheeting.

7 Discussion and conclusions

7.1 General

The objective of this study is to investigate whether a KBS-3 repository for spent nuclear fuel may act as a plane of weakness when subjected to different mechanical loads. Two load cases that could be of concern are studied. These two load cases could theoretically induce shear- and sheet fractures in the repository.

The sensitivity of the rock mass to the presence of a system of tunnels is studied by means of numerical modelling using the two-dimensional distinct element code *UDEC*. In order to study the two load cases listed above, generic static models with schematic assumptions regarding tunnel geometries and loads are analysed. The elastic properties used in the model have similar values to those provided by /Glamheden et al. 2007/ for the rock mass at the Forsmark site. In addition to the static *UDEC* analyses, the results from dynamic earthquake analyses performed by /Fälth et al. 2010/ are used to evaluate the stability during dynamic-induced shearing. The results are summarized below.

7.2 Shearing

7.2.1 Static models

In the static models analysed here, two cases are compared:

- A single fracture embedded in a portion of rock.
- A single fracture embedded in a portion of rock is cutting through a system of tunnel openings, i.e. a repository.

Four different generic *in situ* stress states are considered. The stress anisotropies obtained by the stress states are high. The shear stresses applied along the fracture plane range between 10 and 30 MPa (Figure 5-5, upper). As a reference, it can be noted that according to /Lund et al. 2009/, the shear stresses at the Forsmark site never exceeded 10 MPa during the latest glaciation.

The stability of the fracture is evaluated in terms of the FoS parameter (Factor of Safety). The analysis is based on the initial (before slip) shear- and normal stresses in the fracture, and on bedrock strength parameter values obtained from the Forsmark site investigations /Glamheden et al. 2007/. Besides this, the fracture shear displacement in the hypothetical case of failure is studied. The following conclusions regarding stability and shear displacements can be drawn:

- *Stability:* The results indicate that the stability margin in the fracture has a limited sensitivity to the presence of the tunnels and to the tunnel spacing. Including tunnels with 40 m spacing gives a reduction of the stability margin by about 20% at a maximum. Applying the stress state where the stresses are oriented in order to give maximum instability gives a FoS which is higher than 1.4 for all tunnel spacings larger than 20 m.
- *Shear displacements:* The amount of shear displacement is not influenced by the presence of the tunnels since the behaviour after failure does not depend on the contact area, but merely on the friction properties.

7.2.2 Dynamic models

The stability is evaluated using stress input from generic dynamic earthquake simulations by /Fälth et al. 2010/. The FoS is calculated based on the normal- and shear stresses recorded in horizontal planes in a M_w 6.2 model. Results from two recording points are used. One of the points was located close to the fault edge and thus subjected to specifically large stress redistributions. According to the FoS calculation, the following can be concluded:

- Close to a fault edge, the rock mass may be subjected to loads that induce instability in horizontal planes. This holds irrespective of the presence of tunnels. However, the loads at this location are exaggerated due to the elastic continuum assumption used in the earthquake simulation model and, consequently, the stability evaluation can be regarded overly conservative.
- At the location far from any fault edge, the loads are less exaggerated. Without tunnels the FoS is 4. Including tunnels with 40 m spacing gives a FoS reduction from 4 to 3.5. Reducing the tunnel spacing down to 20 m gives a FoS of 2.

It shall be pointed out that the results are conservative. The stress results were monitored at points located only 200 m from the fault plane. Only a minor part of the repository will be located at such short distances from deformation zones with potential of hosting earthquakes. The major part of the repository will be located at much longer distances where the effects are much less severe /Fälth et al. 2010/. Further, the model, from which the stresses were obtained, simulates an earthquake with high fault slip velocities. It was indicated by the results in /Fälth et al. 2010/ that the fault slip velocity is an important parameter that controls much of the impact on the surrounding rock mass. In addition, the synthetic earthquake has large fault slip given the earthquake magnitude and the continuum in the model is assumed to be linear elastic, which gives exaggerated stress redistributions as the fault slip.

Given the conservative earthquake representation, the results strongly suggest that the repository will not act as a plane of weakness even when subjected to considerable dynamic loads.

7.3 Sheeting

A model with a number of fractures at different depths (10 m, 20 m, 30 m, 40 m, 50 m, 75 m, 100 m and 400 m) is subjected to a horizontal stress increase of 40 MPa in order to provoke tensile fracturing (sheeting). All fractures, both close to the ground surface and at larger depths, follow the ground topography and are assigned zero tensile strength. After the application of the horizontal stress, sheeting (tensile fracturing) is observed in all fractures down to 100 m depth. At 400 m depth, the normal effective stress remains compressive and has been reduced from 6.5 to 6.0 MPa (about 8%).

The 40 MPa stress increase can be regarded as high and thus conservative. The horizontal stress increase due to the glacial load during the latest glaciation is estimated by /Lund et al. 2009/ to have been about 30 MPa. This was at the time of the glacial maximum, i.e. when the vertical stabilizing ice load had its maximum and thus effectively suppressed sheeting. At the time of ice retreat, when the stabilizing ice load had disappeared, the remaining horizontal flexural stresses are estimated to have been of the order of 10 MPa, i.e. 25% of the stress increase assumed here.

Given the conservative model assumptions (a 40 MPa increase in the horizontal compressive stress, fracture geometry that is exactly parallel to the ground topography at all depths and zero fracture tensile strength), it can be concluded that there is no risk of tensile-induced (sheeting) fractures being created below a depth of about 200 m. Hence sheeting fractures occurring at the projected repository depth (about 500 m) is extremely unlikely. Since the vertical stress remains compressive at this depth, a system of tunnels will not increase the risk of tensile-induced fracturing (sheeting).

7.4 Concluding remarks

Based on the findings from the numerical modelling results used in this study, it can be concluded that, for all loading scenarios, the 500-m-deep repository cannot act as a plane of weakness with the deposition tunnel spaced at 40 m. The model results also suggest that reducing the deposition tunnel spacing from 40 m to 20 m will not increase the risk of creating a repository plane of weakness. However, reducing the deposition tunnel spacing to less than 20 m will cause stress interaction between the deposition tunnels. Such deposition tunnel spacing may cause local tunnel overstressing and should be evaluated with the actual repository conditions and properties.

8 References

Ageskog L, Jansson P, 1999. Heat propagation in and around the deep repository. Thermal calculations applied to three hypothetical sites: Aberg, Beberg and Ceberg. SKB TR-99-02, Svensk Kärnbränslehantering AB.

Andersson J C, 2007. Rock Mass Response to Coupled Mechanical Thermal Loading Äspö Pillar Stability Experiment, Sweden, Royal Institute of Technology KTH Architecture and the Built Environment.

Atkinson B K, 1987. Fracture mechanics of rock (Academic Press geology series), Academic Press Limited. ISBN: 0-12-066266-3.

Bahat D, Grossenbacher K A, Karasaki K, 1998. Mechanism of exfoliation joint formation in granitic rocks, Yosemite National Park. Journal of Structural Geology 21(1): pp 85–96.

Brady B H, Brown E T, 1993. Rock Mechanics for underground mining, Chapman & Hall. London, UK.

Carlsson A, 1979. Characteristic features of a superficial rock mass in southern central Sweden – Horizontal and subhorizontal fractures and filling material. Striae 11.

Chan T, Christiansson R, Boulton G S, Eriksson L O, Hartikainen J, Jensen M R, Mas Ivars D, Stanchell F W, Wistrand P, Wallroth T, 2005. DECOVALEX III/BENCHPAR projects. The thermal-hydro-mechanical responses to a glacial cycle and their potential implications for deep geological disposal of nuclear fuel waste in a fractured crystalline rock mass. Report of BMT3/WP4. SKI Report 2005:28, SKI – Statens kärnkraftinspektion (Swedish Nuclear Power Inspectorate) Stockholm Sweden.

Fälth B, Hökmark H, Munier R, 2010. Effects of large earthquakes on a KBS-3 repository. Evaluation of modelling results and their implications for layout and design. SKB TR-08-11 Svensk Kärnbränslehantering AB.

Glamheden R, Fredriksson A, Röshoff K, Karlsson J, Hakami H, Christiansson R, 2007. Rock Mechanics Forsmark. Site descriptive modelling Forsmark stage 2.2. SKB R-07-31, Svensk Kärnbränslehantering AB.

Hökmark H, Lönnqvist M, Fälth B, 2010. THM-issues in repository rock. Thermal, mechanical, thermo-mechanical and hydromechanical evolution of the rock at the Forsmark and Laxemar sites. SKB TR-10-23, Svensk Kärnbränslehantering AB.

Hökmark H, Lönnqvist M, Kristensson O, Sundberg J, Hellström G, 2009. Strategy for thermal dimensioning of the final repository for spent nuclear fuel. Version 1.0. SKB R-09-04, Svensk Kärnbränslehantering AB.

Ikonen K, 2005. Thermal analysis of repository for spent EPR-type fuel. Posiva 2005-06, Posiva Oy Olkiluoto Finland.

Itasca, 2005. *UDEC*, Universal Distinct Element Code, Version: 4. Itasca Consulting Group Inc. Minneapolis, USA.

Jahns R H, 1943. Sheet structure in granites:Its origin and use as a measure of glacial erosion in New England. J. Geol. 51: pp 71–98.

Jing L, Stephansson O, 2007. Fundamentals of Discrete Element Methods for Rock Engineering: Theory and Applications, Elsevier. Amsterdam, The Netherlands. ISBN: 978-0-444-82937-5.

Jonsson M, Bäckström A, Feng Q, Berglund J, Johansson M, Mas Ivars D, Olsson M, 2009. ÄSPÖ Hard Rock Laboratory. Studies of factors that affect and controls the Excavation Damaged/Disturbed Zone. SKB R-09-17, Svensk Kärnbränslehantering AB.

Lund B, Schmidt P, Hieronymus C, 2009. Stress evolution and fault stability during the Weichselian glacial cycle. SKB TR-09-15, Svensk Kärnbränslehantering AB.

Lönnqvist M, Hökmark H, 2010. Assessment of Potential for Glacially Induced Hydraulic Jacking at Different Depths. SKB R-09-35, in prep., Svensk Kärnbränslehantering AB.

Mandl G, 2005. Rock joints. The mechanical genesis, Springer. ISBN: 3-540-24553-7.

Martel S J, 2006. Effect of topographic curvature on near-surface stresses and application to sheeting joints. Goephys. Res. Lett. **33**(L01308).

Martin D, Kaiser P, McCreath D, 1999. Hoek-Brown parameters for predicting the depth of brittle failure around tunnels. Can. Geotechnical Journal 36(1): pp 136–151.

Probert T, Claesson J, 1997. Temperature field due to time-dependent heat sources in a large rectangular grid. Application for the KBS-3 repository. SKB TR 97-27, Svensk Kärnbränslehantering AB.

SKB, 2003. Planning report for the safety assessment SR-Can. SKB TR-03-08, Svensk Kärnbränslehantering AB.

SKB, 2009a. Underground design Forsmark Layout D2. SKB R-08-116, Svensk Kärnbränslehantering AB.

SKB, 2009b. Final repository facility. Underground design premises/D2. SKB R-07-33, Svensk Kärnbränslehantering AB.

SKB, 2010a. Buffer production report. Design, production and initial state of the buffer for the safety assessment SR-Site. SKB TR-10-15, Svensk Kärnbränslehantering AB.

SKB, 2010b. Forsmark Site Engineering Report. Guidelines for Underground Design Step D2. SKB R-08-83, Svensk Kärnbränslehantering AB.

Stephens M B, Fox A, La Pointe P, Simeonov A, Isaksson H, Hermanson J, Öhman J, 2007. Geology Forsmark. Site descriptive modelling Forsmark stage 2.2. SKB R-07-45, Svensk Kärnbränslehantering AB.